

IMPLEMENTATION AND APPLICATION OF
DISPERSION-BASED WAVEGUIDE MODELS FOR
SHALLOW-WATER SONAR PROCESSING

by

OBADAMILOLA ALUKO

BS, Illinois Institute of Technology, 2002

Submitted to the Graduate Faculty of
the School of Engineering in partial fulfillment
of the requirements for the degree of

Master of Science

University of Pittsburgh

2004

UNIVERSITY OF PITTSBURGH
SCHOOL OF ENGINEERING

This thesis was presented

by

OBADAMILOLA ALUKO

It was defended on

December 4, 2003

and approved by

Patrick Loughlin, Professor, Electrical Engineering Department

Luis F. Chapparo, Associate Professor, Electrical Engineering Department

Amro El-jaroudi, Associate Professor, Electrical Engineering Department

Thesis Advisor: Patrick Loughlin, Professor, Electrical Engineering Department

IMPLEMENTATION AND APPLICATION OF DISPERSION-BASED WAVEGUIDE MODELS FOR SHALLOW-WATER SONAR PROCESSING

OBADAMILOLA ALUKO, M.S.

University of Pittsburgh, 2004

In wave propagation, the phenomenon of dispersion, whereby different frequencies travel at different velocities, can result in significant nonstationarities, i.e., time- and spatially-varying characteristics of the wave. This effect is particularly strong in shallow water sound propagation, due to the waveguide-like action of the ocean bottom and surface. These channel-induced nonstationarities can have a deleterious impact on automatic detection and classification in the absence of signal processing techniques that account for dispersive channel effects.

We quantify the effects of dispersion on the spatial and temporal spreading of a propagating wave by considering local temporal, spatial and spectral moments of the modes of the wave. By local moments we mean, for example, the spread (standard deviation) of the wave in time at a particular location; or the average frequency of the wave at a particular time. We implement simple dispersion-based waveguide models of a shallow ocean channel and demonstrate by application to impulsive-source sonar data that simple channel models requiring little environmental information can be used to compensate for the effects of dispersion.

TABLE OF CONTENTS

1.0 INTRODUCTION	1
2.0 BACKGROUND	4
2.1 The Acoustic Wave Equation	4
2.1.1 Solution of the wave equation	5
2.1.2 Ray Theory Solution	6
2.1.3 Normal Mode Solution	8
2.1.4 Multi-path Expansion Solution	10
2.1.5 Fast-Field Solution	10
2.1.6 Range Dependence	11
2.2 Dispersion	12
2.2.1 Dispersion Relation, Phase Velocity and Group Velocity	12
3.0 WAVEGUIDES	16
3.1 2-Plate Waveguide	16
3.1.1 Dispersion relation of the 2-plate waveguide	17
3.1.2 Phase Velocity and Group Velocity of the 2-plate waveguide	19
3.2 Pekeris Waveguide	20
3.2.1 Dispersion relation for the Pekeris Waveguide	22
3.2.2 Phase Velocity and Group Velocity of the Pekeris Waveguide	23
3.2.3 Cut-off for frequencies propagating in the Pekeris Waveguide	25
4.0 IMPLEMENTATION OF WAVEGUIDE MODELS	27
4.1 Dispersion-based Model for Propagation of Sound through Water	28
4.2 Compensation for Dispersion	31
4.3 Implementation of Waveguide Model Using MATLAB	32
4.3.1 2-Plate Waveguide	32
4.3.2 Pekeris Waveguide	33
4.4 Comparing the 2-Plate and the Pekeris Waveguides	35
5.0 APPLICATION OF MODELS TO SONAR DATA	39
6.0 CONCLUSIONS AND FUTURE WORK	44
APPENDIX A. MATLAB CODE FOR PEKERIS WAVEGUIDE FILTER	47
APPENDIX B. GROUP VELOCITY FOR PEKERIS WAVEGUIDE	52

APPENDIX C. MATLAB CODE FOR 2-PLATE WAVEGUIDE FILTER .	56
BIBLIOGRAPHY	60

LIST OF FIGURES

1	Spectrograph of impulse-explosion recorded at 9 km, 19 km and 38 km showing the time-varying spectrum of signals propagating through water (The time axis spans about 0.16 seconds and the frequency range is 0-1000Hz in each plot. [Data courtesy of P. Dahl, APL-UW])	13
2	Schematic for the 2-plate Waveguide, consisting of a water column of depth D meters two perfectly reflecting plates	17
3	Dispersion Curves for modes 1, 2 and 3 for the 2-Plate Waveguide	18
4	Group and Phase Velocity Curves for modes 1, 2 and 3 of the 2-Plate Waveguide, with $c=1500\text{m/s}$ and $D=75\text{m}$	20
5	Cut-off Frequency as a function of depth for modes 1, 2 and 3 of the 2-Plate Waveguide, with $c=1500\text{m/s}$ and $D=75\text{m}$	21
6	Schematic Diagram of the Pekeris Waveguide	21
7	Dispersion Curves for modes 1, 2 and 3 for the Pekeris Waveguide. Model parameters are $c_1 = 1500\text{m/s}$, $c_2 = 1800\text{m/s}$, $\rho_1 = 1000\text{kg/m}^3$, $\rho_2 = 1800\text{kg/m}^3$ and $D=75\text{m}$	23
8	Group and Phase velocity Curves for modes 1, 2 and 3 for the Pekeris Waveguide, Model parameters are $c_1 = 1500\text{m/s}$, $c_2 = 1800\text{m/s}$, $\rho_1 = 1000\text{kg/m}^3$, $\rho_2 = 1800\text{kg/m}^3$ and $D=75\text{m}$	25
9	Cut-off as function of Depth for mode 1 of the 2-Plate and Pekeris Waveguide	26
10	The local and global moments of the spectrum of a signal	28
11	Frequency response of 2-plate waveguide of depth 50m at 10km	31
12	Spectrograph of Pekeris Waveguide and 2-Plate Waveguide at depth of 3m	36
13	Spectrograph of Pekeris Waveguide and 2-Plate Waveguide at depth of 10m.	37
14	Spectrograph of Pekeris Waveguide and 2-Plate Waveguide at depth of 50m.	38
15	Cut-off frequency vs. Depth for 2-plate and Pekeris waveguides.	38
16	Speed profile for Yellow sea and experimental setup for measurements of data.	40

17	Comparing signals recorded at sea with simulated signals for the Pekeris waveguide: The double pulse in the measured data is caused by air bubbles formed from the initial explosion	41
18	Comparing signals recorded at sea with the corresponding filtered signal for the Pekeris waveguide	42
19	Comparing signals recorded at sea with the corresponding filtered signal for the Pekeris waveguide (Recorded signals above and the filtered signals below: The bubble pulse is clearly evident in the time-series of the filtered data). . .	43
20	Figure showing example of range and depth dependence: the depth changes with range and the sound speed profile varies with depth.	45

1.0 INTRODUCTION

Ocean acoustics is the science of sound in the sea and deals with both the study of sound propagation and the recovery of sound from interfering acoustic phenomena such as dispersion.

Waveguides direct the flow of signals and allow for the propagation of the signals through a medium. They form a path for which waves are guided through a medium. The ocean acts as a horizontally stratified waveguide for sound propagation with its surface and bottom as boundaries e.g [22]. Shallow-water waveguides and deep-water waveguides have clearly different characteristics. However, the classification between both types of propagation is relative and is dependent on the product of the horizontal wavenumber and depth. In this thesis, we focus on shallow water, where dispersive effects are prominent.

In an ideal waveguide, there is total reflection without any loss in energy as the sound hits the boundaries of the waveguide. The perfect homogeneous waveguide models the ocean in the simplest ideal case as two rigid and smooth parallel plates representing the ocean surface and bottom. Another ideal, but more complex waveguide, is the two-layered waveguide. This waveguide consists of a homogeneous layer of water overlaying a denser medium [21][22]. Pekeris was the one who thought to model the ocean as a waveguide.

The acoustic wave equation is a result of linear approximations to the hydrodynamic equations [20]. This equation can be used to relate different parameters of the ocean such as pressure, particle velocity, velocity potential and displacement potential to changes in time and distance. However, the acoustic wave equation has the same form regardless of what parameter is used. This equation will be the basis of the models developed in this thesis.

To understand and compensate for the dispersive effects of shallow-water propagation of sound, a waveguide model of the ocean channel is useful. A dispersion-based waveguide

model can be generated with a proper relation for both the group velocity and phase velocity to the frequency of the propagating signals. With the phase velocity, the vertical wavenumber can be obtained and this can be used to eventually generate the group velocity. With the group velocity, it is possible to generate the group delay of the signal at every frequency and then make up for that delay in time.

Modeling is essential in providing a proper method for investigating the performance of hypothetical sonar designs under varied environmental conditions as well as to estimate the performance of existing sonars in different ocean areas and seasons. Researchers use modeling to simulate sonar performance in the ocean using laboratory conditions. Modeling is of two distinct categories. Physical models, sometimes referred to as analytic models, are concerned with the theoretical or conceptual representation of the physical processes occurring in the ocean. An example is a tank used to model the ocean. Mathematical models refer to models based on both observation and mathematical representations of the processes occurring in the ocean.

Mathematical models are sub-categorized into Environmental models, Basic Acoustic models and Sonar performance models. Environmental models are implemented using algorithms, based on observation, that are used to quantify the boundary conditions and volumetric effects of the ocean environment. They also make use of parameters such as the sound speed, medium density, absorption coefficients, and surface and bottom reflection losses. The models discussed in this thesis are environmental mathematical models utilizing a minimal number of these environmental factors.

The models developed here will eventually be applied to sonar systems that are used for detection and classification of signals. With the effects of dispersion on propagating signals, the automatic detection and classification is very difficult and inaccurate. By taking into consideration the dispersive effects of the ocean channel, we account for dispersion in the processing of the signals so that detection and classification by the sonar systems potentially becomes more efficient and accurate.

We will start the discussion by first defining basic terms used to describe waves and introduce concepts that form the foundation of the propagation models proposed. After establishing the basic concepts, the propagation models are introduced and a thorough de-

scription of them is provided. Finally, applications of the models to real and simulated data are presented and a comparison of the two models with each other, and also with other types of models are made.

Some Definitions and Notation

sound speed, c : The speed of sound in water without any boundary conditions (in m/s).

phase velocity, v : The speed at which the phase of a sinusoid travels in water (in m/s).

This is dependent on frequency in dispersive channels.

group velocity, u : This is the speed of points of constant amplitude (in m/s). It is also referred to as the rate of energy transfer and is also dependent on frequency in dispersive channels.

wavenumber, κ : The number of wavelengths in 2π units of length of a signal (in $rads/m$).

In dispersive media, this quantity is dependent on frequency.

2.0 BACKGROUND

2.1 THE ACOUSTIC WAVE EQUATION

The acoustic wave equation is a result of linear approximations to the wave equation ¹. The wave equation is derived from the more fundamental equations of state, continuity and motion. It is a mathematical depiction of the behavior of different properties such as pressure and velocity as they vary with time or space. There are wave equations for pressure, particle velocity, velocity potential and displacement potential. They all have the same form but focus will be given to the wave equation for pressure, which is:

$$\nabla(\nabla^2\Phi - \frac{1}{c^2}\frac{\partial^2\Phi}{\partial t^2}) = 0 \quad (2.1)$$

Equation (2.1) is satisfied when

$$\nabla^2\Phi - \frac{1}{c^2}\frac{\partial^2\Phi}{\partial t^2} = 0, \quad (2.2)$$

where

$$\nabla^2 = \frac{\partial^2}{\partial x^2} + \frac{\partial^2}{\partial y^2} + \frac{\partial^2}{\partial z^2}$$

in Cartesian coordinates and

$$\nabla^2 = \frac{\partial^2}{\partial r^2} + \frac{1}{r}\frac{\partial^2}{\partial y^2} + \frac{\partial^2}{\partial z^2}$$

in cylindrical coordinates.

Φ is the pressure of the propagating wave and c is the speed of sound. This equation forms the foundation of all mathematical models of acoustic propagation.

¹Sources: [11], [13], [14], [27]

2.1.1 Solution of the wave equation

For a single frequency, the harmonic (single-frequency) velocity potential solution for the wave equation is:

$$\Phi = \phi e^{-j\omega t}, \quad (2.3)$$

where ϕ is the time independent potential function and ω is the source frequency (in radians). Using this solution, the wave equation then reduces to

$$\nabla^2 \phi + \frac{\omega^2}{c^2} \phi = 0. \quad (2.4)$$

This result is the Helmholtz equation, which is time-independent. Therefore it is referred to as the time-independent wave equation.

There is no universal solution technique to the wave equation. However, the Helmholtz equation would be used as the new simplified wave equation from which solutions would be derived. There are different methods for which a solution to the Helmholtz equation can be derived. The method of choice is dependent on a number of factors, the most important being the following:

- Boundary Conditions
- Complexity of the Ocean properties
- Frequency and Bandwidth of the Propagating Sound
- Geometrical Assumptions of the Ocean

The different methods for obtaining a solution are outlined in the following section.

The aim of the modeling in this research is to model the propagation of sound in the ocean accurately using as few properties of the ocean as possible. The option for the solution to the acoustic wave equation would rely on very few medium properties. The method of choice for the models in this thesis is the Normal mode solution where only the speed of sound, densities of the mediums and depth are required.

2.1.2 Ray Theory Solution

The Ray theory solution is based on ray-tracing. The assumption is made that the time-independent solution of the Helmholtz equation, ϕ , is in the form of a product of an amplitude function and a phase function.

$$\phi = \mathbf{A}e^{-jP(x,y,z)}, \quad (2.5)$$

where $\mathbf{A} = \sum_{i=0}^{\infty} A_i(x, y, z)$ and is referred to as the ray series.

After taking the derivatives of ϕ to get the gradients, substituting them into the Helmholtz equation and then collecting like terms (real and imaginary), we obtain:

$$\begin{aligned} \nabla\phi &= \nabla\mathbf{A}e^{jP} + j\mathbf{A}\nabla Pe^{jP} \\ \nabla^2\phi &= \nabla^2\mathbf{A}e^{jP} + j2\nabla\mathbf{A}\nabla Pe^{jP} + j\mathbf{A}\nabla^2Pe^{jP} - \mathbf{A}[\nabla P]^2e^{jP} \end{aligned}$$

and

$$\left(\frac{1}{\mathbf{A}}\right)\nabla^2\mathbf{A} - [\nabla P]^2 + \left(\frac{\omega}{c}\right)^2 = 0 \quad (2.6)$$

$$2\nabla\mathbf{A}\nabla P + \mathbf{A}\nabla^2P = 0 \quad (2.7)$$

Assuming that the amplitude function varies much slower with position than the phase function does and that the gradient of the amplitude is small compared to the ratio of the frequency and speed, we can simplify equation (2.6) to:

$$[\nabla P]^2 = \left(\frac{\omega}{c}\right)^2 = \kappa^2 \quad (2.8)$$

for $\left(\frac{1}{\mathbf{A}}\right)\nabla^2\mathbf{A} \ll \kappa^2$, where κ is the wavenumber. This is a high-frequency approximation of the equation. This equation(2.8) is called the eikonal equation and since it is independent of the amplitude function, it is easily used to find the phase function of ϕ . By making the coordinate system spherical, the eikonal equation becomes

$$\left[\frac{\partial P}{\partial s}\right]^2 = \kappa^2 \quad (2.9)$$

and

$$P(s) = P(0) + \int_0^s \kappa^2 ds'. \quad (2.10)$$

where s is the distance along a ray from the point source. Surfaces of constant phase are called wavefronts while their normals are called rays.

\mathbf{A} is an infinite series and its application to equation (2.7) results in an infinite number of equations. These equations are referred to as the transport equations and they determine the wave amplitudes. Due to the high frequency approximation made earlier, only the first transport equation would be considered to find the amplitude associated with each wave. This is:

$$2\nabla P \nabla A_0 + (\nabla^2 P) A_0 = 0. \quad (2.11)$$

In spherical coordinates, the solution to the transport equation can be easily solved for and is obtained as

$$A_0(s) = A_0(0) \sqrt{\frac{c(s)J(0)}{c(0)J(s)}}. \quad (2.12)$$

$J(s)$ is the cross-section of the ray bundle at a distance s from the point source and $c(s)$ is the speed along the ray at distance s .

The Ray Theory solution is most efficient and accurate at high frequencies and in deep waters, [24]. The distinction between shallow water propagation and deep water propagation is dependent on the dimensionless parameter κh , where κ is the horizontal wavenumber (spatial frequency) and h being the water depth. Usually, small values of κh ($\kappa h \leq 10$) are representative of shallow water, whereas large κh values occur designate deep water, [26]. Propagation of sound in shallow water is characterized by repeated interactions with the sea floor and water surface. Generally, coastal waters of depth of not more than 150m are considered as shallow. Although again, in terms of propagation effects on the wave, the designation of "shallow" is frequency dependent. In shallow coastal waters, the water layer is often homogeneous so it is appropriate to assume that the average value of sound speed is constant. It is also appropriate to assume a constant density for the ocean water.

2.1.3 Normal Mode Solution

The practicality of this method of solution is based on the assumption of a cylindrical symmetry in a stratified medium. The solution is derived from an integral representation of the wave equation and is a product of a function of depth and another function of range. Therefore:

$$\phi = A(z)B(r) \quad (2.13)$$

It should be noted that the changes in the properties of the medium are with depth only (range independence) ².

Plugging ϕ into the Helmholtz equations and using k_{rm}^2 as a separation variable, the following results are obtained:

$$\frac{\partial^2 A}{\partial z^2} + (\kappa^2 - \kappa_{rm}^2)A = 0 \quad (2.14)$$

$$\frac{\partial^2 B}{\partial r^2} + \frac{1}{r} \frac{\partial B}{\partial r} + \kappa_{rm}^2 B = 0 \quad (2.15)$$

Equation (2.15) is the range equation and it describes the traveling wave portion of the solution. It is the zero-order Bessel equation and its solution is in the form of a zero-order Hankel function ($H_0^{(1)}$). Equation (2.14) is the depth equation and it describes the standing wave portion of the solution. The solution of a standing wave equation is called a mode and the solution to the depth equation is called the Green's function, so the Green's function is made up of modes of the wave. Each normal mode is a traveling wave in the horizontal direction and a standing wave in the vertical direction. The full solution of ϕ can be expressed by an infinite integral assuming a point source:

$$\phi = \int_{-\infty}^{\infty} \mathbf{G}(z, z_0; \kappa_{rm}) \cdot \mathbf{H}_0^{(1)}(\kappa_{rm} r) \kappa_{rm} d\kappa_{rm} \quad (2.16)$$

where \mathbf{G} is the Greens function and $\mathbf{H}_0^{(1)}$ is a zero-order Hankel function of the first kind.

The infinite integral in equation (2.16) can be simplified by considering two types of modes that propagate through the medium. They are the trapped or discrete modes and

²see section 2.1.6

the continuous modes. The discrete modes propagate through the water layer of a stratified medium while the continuous modes propagate through the ocean floor.

In the infinite integral, the discrete modes are represented by a contour integral of the same functions (Green and Hankel) and the continuous part is whatever is left of the infinite integral, [20]. The result is:

$$\phi = \oint \sum_{m=1}^{\infty} \frac{A_m(z_0)A_m(z)}{\kappa^2 - \kappa_{rm}^2} \mathbf{H}_0^{(1)}(\kappa_{rm}r) \cdot \kappa_{rm} d\kappa + Cont. \quad (2.17)$$

$$A_m(z) = \sqrt{\frac{2\rho}{z}} \sin(\kappa_{rm}z) \quad (2.18)$$

κ_{rm} is an eigenvalue of the Green's function and the corresponding eigenfunction is $A_m(z)$. Note that in equations (2.17) and (2.18), $A_m(z_0)$ is the eigenfunction calculated at the depth of the source. Here, the assumption is made that the source and receiver are at the same depth.

The simplification of the infinite integral is justified in shallow water because the continuous modes are negligible at distances of propagation that are greater than multiples of the water depth. Eventually, the infinite integral in equation (2.16) is approximated by the contour integral (neglecting the continuous modes), although there are still an infinite number of discrete modes present. The contour is the cylinder with a radius of the same length as the distance of propagation and with a height the same as the water depth.

The Hankel function can be asymptotically expanded resulting in an estimate for the first order (which is a far-field approximation when $\kappa r \gg 1$) that is:

$$\mathbf{H}_0^{(1)}(\kappa_{rm}r) \approx \sqrt{\frac{2}{\pi \kappa_{rm}r}} e^{j(\kappa_{rm}r - \pi/4)}. \quad (2.19)$$

The solution for ϕ obtained from all the approximations above is:

$$\phi = \frac{\sqrt{2\pi\kappa_0}}{\rho_s} \sum_{m=1}^{\infty} \frac{A_m(z_0)A_m(z)}{\kappa_{rm}} e^{j(\kappa_{rm}r - \pi/4)} e^{\kappa_0} \quad (2.20)$$

$$(2.21)$$

where ρ_s is the density of the water medium at the source of the wave and $\kappa_0 = \omega/c$ is the wavenumber at the source. The continuous modes are analogous to rays (in ray theory) that strike the ocean floor at angles greater than the critical angle.

The normal mode solution is most efficient for low frequency propagation, especially in shallow waters. The efficiency is limited to low frequencies because the number of modes required for proper prediction in computational models is proportional to the frequency. It requires a large number of modes to properly predict propagation at high frequencies than it takes to properly predict the propagation at low frequencies.

Of all the techniques used to solve the wave equation, the normal mode solution is the only one that accounts for dispersion by utilizing the dispersion relation in it. It is the only solution that gives the wavenumber as part of its solution, relating κ and ω .

2.1.4 Multi-path Expansion Solution

The multipath expansion technique is a combination of the normal mode technique and the ray theory method. Therefore, it is a hybrid model. It is efficient in modeling propagation at high and intermediate frequencies, usually in deep waters.

The solution derived from this method is in the form of a depth function and a range function, as in the normal mode method. However, the multi-path expansion technique expands the infinite integral representation (equation (2.16)) of the normal mode solution in terms of a set of infinite integrals, each of which is associated with a particular ray path. Therefore, each normal mode can be represented by corresponding rays but only certain modes are considered.

2.1.5 Fast-Field Solution

The Fast-Field solution is of the form of the normal mode approach. However, the infinite integral is evaluated by means of the Fast Fourier Transform (FFT). The solution obtained is still a complicated one but simplifications can be made by approximations to the Green's function. A proper derivation of this can be found in [20],[27].

2.1.6 Range Dependence

Range dependence of a waveguide model exists when some properties of the ocean change as a function of the range from the receiver, in addition to changes resulting from depth dependence. Some of the properties that could change with range are the sound speed, density and temperature in the water. Range independence on the other hand indicates that the changes in the properties of the ocean are functions of depth only and do not change with range. This implies a constant depth of the ocean, regardless of the distance from the source, and the convenience of using the cylindrical coordinate system.

Range dependence can be classified as 2-dimensional or 3-dimensional. In 2-dimensional range dependence, the properties of the ocean usually vary as a function of depth and range from the source only. 3-dimensional range dependence exists when the properties of the ocean vary as a function of depth, range and azimuth. The azimuth is the angle of incidence of the wave. It is usually the angle of propagation from the horizontal axis.

The different models described in the previous section can be further classified into range-dependent or range-independent models. The normal mode, fast field and multi-path expansion models are range-independent models. However, the normal mode model can be converted to a range-dependent model by mode coupling, [20]. By doing this, the energy transferred from one mode to others has to be considered. Alternatively, if the environmental changes are gradual, one could assume that all the energy in one mode transfers completely into the corresponding mode in the new environment.

Although it is theoretically possible to introduce a 3-dimensional range dependence to ray theory model techniques, however it is very rigorous to implement and is rarely done. A significant problem that confronts range dependence is the proper representation of the transition of sound speed profiles as it changes with range. The mathematical complexity discourages 3-dimensional problems in favor of 2-dimensional problems.

2.2 DISPERSION

Dispersion is a phenomenon in which the propagation velocity of a signal is dependent on the frequency of the signal. If a signal with different frequency components is propagated through water, each frequency component would have a different group velocity and so would take different intervals of time to reach a receiver from a source at a distance. The effect of dispersion on a sound signal is that the sound heard at a point would be different from the sound heard at a further distance from the source. There are two types of dispersion: geometric or structural dispersion arising from the waveguide-like action of the ocean surface and the bottom; and material dispersion due to the medium. In shallow water, structural dispersion is dominant and its effects are most obvious at lower frequencies ($f < 500 \text{ Hz}$) and shallow depths³.

The time-frequency distributions in Figure 1 show how the spectrum of a signal changes with time and distance. The initial signal is an impulse explosion. The signal is observed at distances of 9km, 19km and 38km from the source of the explosion. The spectrograph of the signal obviously changes with distance when compared to the original signal. The effects of dispersion become more pronounced as the signal travels further. Notice how the higher frequencies are unaffected at the various distances but the lower frequencies become more hooked. This is a result of the dispersive effects of the shallow ocean.

In a water medium acting as a waveguide, dispersion is a result of the characteristics (such as density) and geometry (depth and range) of the waveguide and is different from basic dispersion such as the occurrence when light passes through a prism and is split into its different components.

2.2.1 Dispersion Relation, Phase Velocity and Group Velocity

An expression that relates the frequency, ω , to the wavenumber, κ , of a medium is called a dispersion relation⁴. This is where the use of the Normal mode solution⁵ of the wave equation

³also see [10][16][24]

⁴see [14], [26], [27]

⁵Normal mode solution is covered in chapter 4, and references [3] and [15]

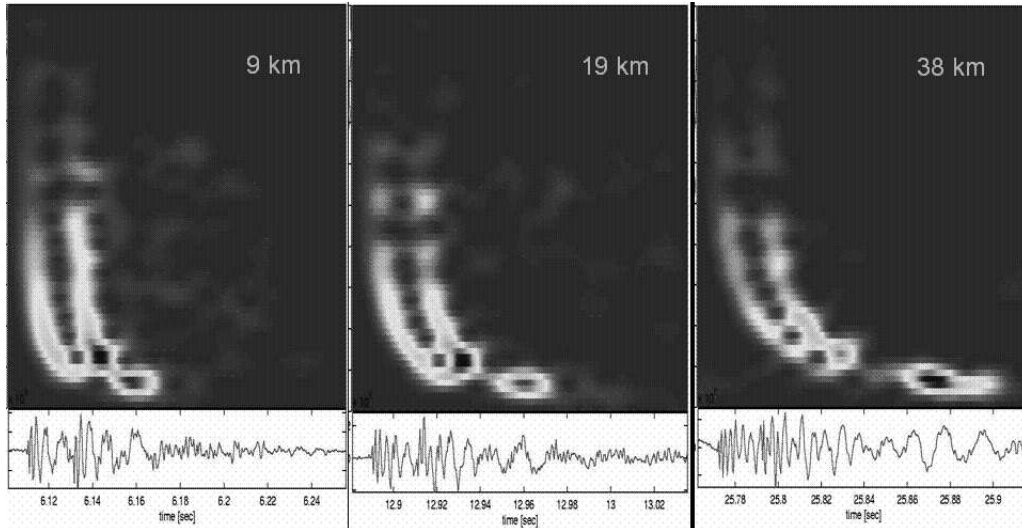


Figure 1: Spectrograph of impulse-explosion recorded at 9 km, 19 km and 38 km showing the time-varying spectrum of signals propagating through water (The time axis spans about 0.16 seconds and the frequency range is 0-1000Hz in each plot. [Data courtesy of P. Dahl, APL-UW])

is useful, because it relates the dispersion relation to the solution of the wave. The plot of frequency versus wavenumber is referred to as a dispersion curve. In the non-dispersive case, the dispersion curve is a straight line through the origin, given by:

$$\kappa = 2\pi/\lambda = \omega/c, \quad (2.22)$$

as in [23] where λ is the wavelength, ω is the frequency in radian and c is the speed of sound in an ideal medium.

The medium wavenumber can be broken into a horizontal and vertical component

$$\kappa = \sqrt{\kappa_z^2 + \kappa_r^2},$$

where κ_z is the vertical component and κ_r is the horizontal component. Since we will be dealing with propagation in the horizontal direction, our focus will be on the horizontal wavenumber of the medium. In non-dispersive mediums the wavenumber is equivalent to the horizontal wavenumber. The vertical wavenumber is zero. So $\kappa_r = \kappa = \omega/c$.

The relation between ω and κ determines the phase and group velocities of the signal. The feature of dispersion is the variation of velocity with frequency (or wavelength). The phase velocity of a sinusoidal signal is the distance the signal with a particular phase travels in a second. This velocity represents the horizontal velocity of a particular phase. The phase velocity of a particular mode of a signal is related to the horizontal wavenumber of the medium by:

$$v_m = \frac{\omega}{\kappa_{rm}} \quad (2.23)$$

where $m = 1, 2, \dots$ is the mode number.

The value of phase velocity is positive if the propagation is in the positive horizontal direction and is negative if the direction of propagation is in the negative horizontal direction. Propagation in the models here are assumed to be in the positive horizontal direction. The phase velocity is always larger than the velocity of sound in the medium, c , but it approaches this velocity for increasing frequencies (where dispersion is not that significant).

The different frequency components of a signal form groups⁶. In dispersive media, these groups travel at different speeds, called the group velocity. Usually as the signal propagates the group will be smeared out and may eventually disappear. If it were a non-dispersive medium, the phase velocity and group velocity would be equal. The group velocity is also referred to as the energy transport velocity, which is the rate at which the energy in the signal travels. The group velocity of a signal for a particular mode is related to the vertical wavenumber by:

$$u_m = \frac{d\omega}{d\kappa_{rm}} \quad (2.24)$$

The signal carried by mode m will propagate with the horizontal speed u_m , which is the slope of the dispersion curve.

The phase velocity of a mode, v_m , is the velocity of points of constant phase angle. The group velocity is the velocity of points of constant amplitude. Both can be derived from the dispersion relation. To conclude, a dispersive medium will propagate a single frequency signal with a phase velocity that depends on the frequency. A signal with multiple frequency

⁶see [4] and [25]

components will also be propagated with varying phase velocities and the shape of the signal will definitely be changed.

When a signal propagates through water, there is a clear difference in the time-varying spectra of the signal measured at various distances from the source (Figure 1). These spectra are shown as time-frequency distributions $P(t, \omega)$. The time-frequency distribution of a signal can be obtained through various different methods. Two of these methods are the Short-Time Fourier Transform (STFT)[2] and the Wigner Distribution. Both of these methods are covered in the Appendix.

3.0 WAVEGUIDES

As stated in the Introduction, two types of waveguides are of interest in ocean acoustics. These are the 2-plate and the Pekeris waveguides. They are both layered media waveguides but the difference between them is in the medium underlying the water column. The following sections describe both waveguides in more detail.

3.1 2-PLATE WAVEGUIDE

The 2-plate waveguide is also referred to as the Ideal Fluid waveguide [6],[26]. It is the simplest model of the ocean waveguide. It is a range-independent, isovelocity water column with perfectly reflecting water surface and sea bottom. Isovelocity means that the sound speed profile is constant and independent of depth. Figure 2 shows a schematic of the 2-plate waveguide with the water surface at $z = 0$ and sea bottom at $z = D$.

The presence of the boundary at $z = D$ requires that the following condition be satisfied

$$\kappa_{zm}D = m\pi \quad m = 1, 2, \dots \quad (3.1)$$

where κ_{zm} is the vertical wavenumber for mode m . This result limits the permissible values of κ_{zm} to a discrete set corresponding to the integer values of m . Therefore, the κ_z spectrum is discrete. If there is no boundary at $z = D$ such that the waveguide represents an infinite half-space, the solution is still the same but it is without limitations on the value of κ_z . The κ_z spectrum is therefore continuous. This can be achieved by making $D \rightarrow \infty$, i.e. by moving the lower boundary to great depths.

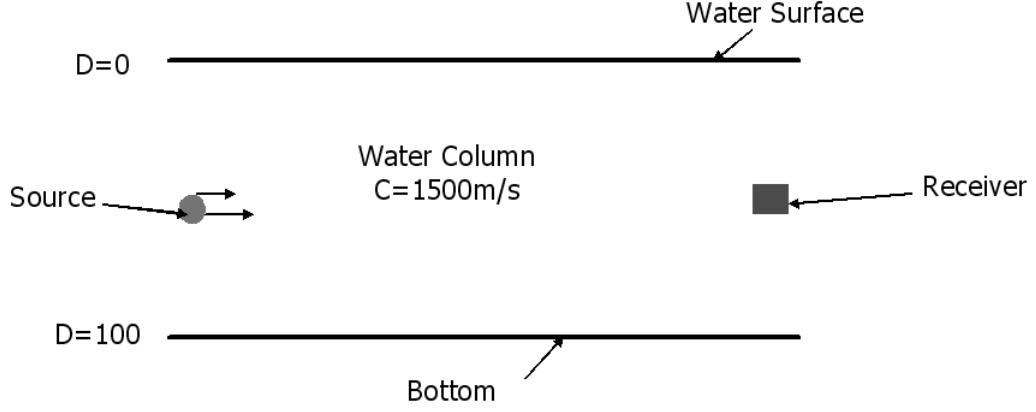


Figure 2: Schematic for the 2-plate Waveguide, consisting of a water column of depth D meters two perfectly reflecting plates

3.1.1 Dispersion relation of the 2-plate waveguide

¹Under the assumption that both boundary conditions of the 2-plate waveguide are free, the characteristic equation for the wave equation that satisfies the boundary conditions is:

$$\kappa_{zm}D = m\pi \quad m = 1, 2, \dots$$

If there is a rigid boundary as in the case of the model of the ocean as a 2-plate waveguide, the characteristic equation that satisfies the boundary conditions is:

$$\kappa_{zm}D = \left(m - \frac{1}{2}\right)\pi \quad m = 1, 2, \dots \quad (3.2)$$

where κ_{zm} is the vertical wavenumber of the m^{th} mode. The resultant wavenumber of the medium is a sum of the horizontal and vertical component:

$$\kappa_m^2 = \kappa_{zm}^2 + \kappa_{rm}^2 = \frac{\omega^2}{c^2},$$

$\omega = 2\pi f$ is the angular frequency. We are interested in the horizontal propagation of the wave. So if we solve for the horizontal wavenumber in terms of the frequency, we would

¹see [14],[26],[27]

end up with the dispersion relation for the 2-plate waveguide, according to the following derivation.

$$\kappa_{rm}(\omega) = \frac{1}{c} \sqrt{\omega^2 - \left(\frac{(m - \frac{1}{2})\pi c}{D}\right)^2} \quad (3.3)$$

$$\omega(\kappa_{rm}) = c \sqrt{\kappa_{rm}^2 + \left(\frac{(m - \frac{1}{2})\pi}{D}\right)^2} \quad (3.4)$$

Equations (3.3) and (3.4) are the dispersion relation for the 2-plate waveguide. The dispersion curves are a set of hyperbolas, each corresponding to a particular mode. Figure 3 below shows the dispersion curves for the first three modes.

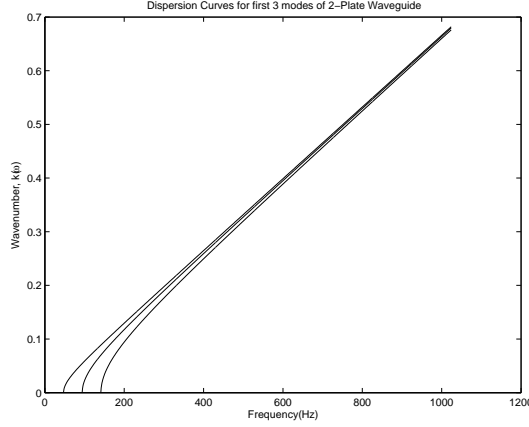


Figure 3: Dispersion Curves for modes 1, 2 and 3 for the 2-Plate Waveguide

Note that there exist a minimum frequency for which these equations can be used. This minimum frequency is called the cut-off frequency; frequencies below this cut-off do not propagate with any significant energy. The m^{th} mode low-frequency cut-off is given by:

$$\omega_{0m} = \frac{(m - \frac{1}{2})\pi c}{D} \quad (3.5)$$

Only frequencies greater than this cut-off frequency have significant amplitude during propagation in the ocean. Frequencies below this cut-off have exponentially decaying amplitude and are insignificant to consider for propagation.

3.1.2 Phase Velocity and Group Velocity of the 2-plate waveguide

Points of constant phase travel with the speed of $v_m = \frac{\omega}{\kappa_{rm}}$. This is the phase velocity in the horizontal direction for mode m . By using the dispersion relation given above for the 2-plate waveguide, the resulting phase velocity is:

$$v_m = \frac{\omega c}{\sqrt{\omega^2 - \left(\frac{(m-\frac{1}{2})\pi c}{D}\right)^2}}. \quad (3.6)$$

Different phase components in a signal combine to form groups. This signal is a series of groups with varying amplitude (due to cancelations and additions). A group maximum corresponds to a point where all neighboring components are in phase. The velocity at which this group maximum travels from one point to another is called the group velocity and it is given as

$$u_m = \frac{\partial \omega}{\partial \kappa_{rm}} = \frac{\kappa_{rm} c}{\sqrt{\kappa_{rm}^2 + \left(\frac{(m-\frac{1}{2})\pi}{D}\right)^2}}. \quad (3.7)$$

$$(3.8)$$

By substituting for κ_{rm} per (3.3), we can next express the group velocity in terms of frequency ω ,

$$u_m = \frac{c \sqrt{\omega^2 - \left(\frac{(m-\frac{1}{2})\pi c}{D}\right)^2}}{\omega} = c \sqrt{1 - \left(\frac{\omega_0 m}{\omega}\right)^2} \quad (3.9)$$

Figure 4, shows the phase velocity and group velocity curves for the first three modes of the 2-plate waveguide.

Note how the group velocity is always less than the speed of sound in an ideal medium and the phase velocity is always greater than it. From the equation for the group velocity, there is a limit to the values that it can have. As the frequency tends to infinity, the group velocity tends to c , which is the speed of sound in an ideal medium. The group velocity tends to zero as the frequency tends to $\frac{m\pi}{D}$. The phase velocity ranges from c to infinity. The value tends to c as the frequency tends to infinity.

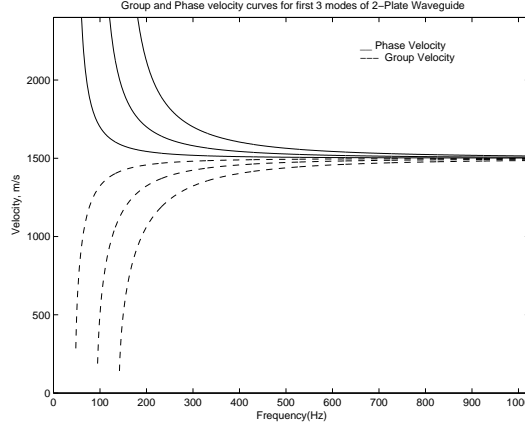


Figure 4: Group and Phase Velocity Curves for modes 1, 2 and 3 of the 2-Plate Waveguide, with $c=1500\text{m/s}$ and $D=75\text{m}$

The group velocity and phase velocity of a wave are related to the angle of incidence of the wave. The relation is as follows

$$u_m = c \sin\theta_m = \frac{c}{\omega} \sqrt{\omega^2 - \omega_{0m}^2}$$

$$v_m = \frac{c}{\sin\theta_m} = \frac{c\omega}{\omega^2 - \omega_{0m}^2}.$$

At the cut-off, the phase velocity tends to infinity while the group velocity tends to zero, corresponding to an angle of incidence of the wave equal to zero. As $t \rightarrow \infty$ the arrival frequency tends to cutoff and the group velocity vanishes. For this reason, the frequency at cut-off takes forever to travel.

Figure 5 shows how the cut-off varies with depth for different modes.

3.2 PEKERIS WAVEGUIDE

The Pekeris waveguide [21][22] models the ocean as a homogeneous layer of water overlying a fluid half-space. The sound velocity in the water layer is c_1 while the sound velocity in the underlying fluid half-space is c_2 , with $c_2 > c_1$. The water surface is at $z = 0$ and the water-fluid boundary is at $z = D$, where D is the depth of the water layer. The surface layer

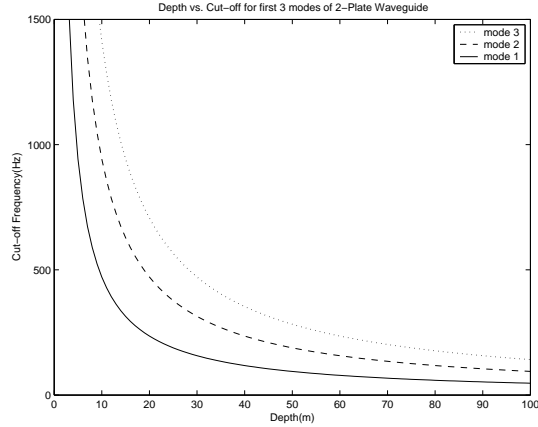


Figure 5: Cut-off Frequency as a function of depth for modes 1, 2 and 3 of the 2-Plate Waveguide, with $c=1500\text{m/s}$ and $D=75\text{m}$

acts as a perfect reflector for waves with an angle of incidence greater than the critical angle in Ray theory ($\theta > \theta_c$). The Pekeris waveguide is sort of an idealized model like the 2-plate waveguide but the complexity is higher than that of the 2-plate waveguide,(see Figure 6). It is sometimes referred to as the partial or imperfect waveguide. This model has met with success and is useful in explaining properties of explosion-generated sound in coastal waters.

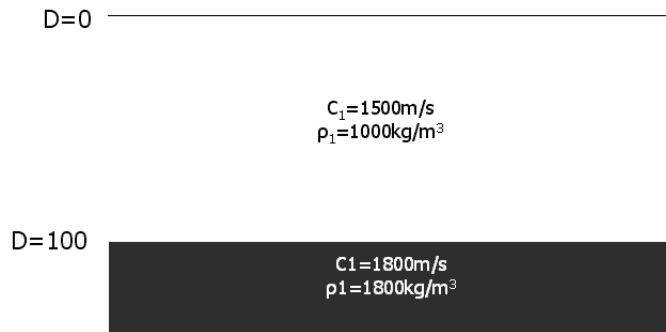


Figure 6: Schematic Diagram of the Pekeris Waveguide

In the Pekeris waveguide, the density of the fluid half-space (ρ_2) is greater than that of water (ρ_1). Typical values for density of water range from $\rho = 1000 - 1030\text{kg/m}^3$. Some bottom densities are: Earth's crust = 2800kg/m^3 and granite = 2700kg/m^3 .

3.2.1 Dispersion relation for the Pekeris Waveguide

The dispersion relation for the Pekeris waveguide is not as simple as that for the 2-plate waveguide. Instead of a single relation between the wavenumber and frequency (as in the 2-plate case), we have a sequence of equations that relate the two parameters [26].

For the boundary condition at $z = D$ to be satisfied, the characteristic equation for the wave equation is:

$$\kappa_{zm1}D + \text{Arctan}\left(\frac{1}{a} \frac{\kappa_{zm1}}{g_2}\right) = m\pi \quad (3.10)$$

$$(3.11)$$

where $a = \frac{\rho_1}{\rho_2}$ and κ_{zm1} is the vertical wavenumber of the m^{th} mode in the water medium. Since we are investigating horizontal propagation, we are concerned with the horizontal wavenumber of the medium. This can be calculated from the resultant wavenumber, $\kappa = \frac{\omega}{c}$, of the medium and the vertical wavenumber κ_{zm} . The vertical wavenumber of the underlying fluid layer is also put into consideration. This will be referred to as g_2 , as in equation (3.8).

The vertical wavenumber of the water medium κ_{zm1} is related to the vertical wavenumber as

$$\kappa_{zm1} = \sqrt{\left(\frac{\omega^2}{c_1^2} - \kappa_{rm1}^2\right)} = \kappa_{rm1} \sqrt{\left(\frac{v_m^2}{c_1^2} - 1\right)}. \quad (3.12)$$

By considering phase velocities between c_1 and c_2 , the vertical wavenumber of the fluid layer is

$$g_{zm2} = \sqrt{\left(\kappa_{rm1}^2 - \frac{\omega^2}{c_1^2}\right)} = \kappa_{rm1} \sqrt{\left(1 - \frac{v_m^2}{c_1^2}\right)}. \quad (3.13)$$

The reason why we use κ_{rm1}^2 is that it represents the portion of the wave that is reflected back into the water medium. It is the imaginary part of the wavenumber of the underlying medium ². Substituting these in the characteristic equation yields

$$\kappa_{rm1}D \sqrt{\frac{v_m^2}{c_1^2} - 1} = m\pi - \text{Arctan}\left[\frac{1}{a} \sqrt{\frac{\frac{v_m^2}{c_1^2} - 1}{1 - \frac{v_m^2}{c_2^2}}}\right].$$

²(“*Ocean Acoustic*” by Tolstoy and Clay gives a more detailed description)

This function gives a relationship between the horizontal wavenumber and the phase velocity of the wave. This equation is

$$\kappa_{rm1} = \frac{1}{\sqrt{\frac{v_m^2}{c_1^2}}} \left[\frac{m\pi}{D} - \frac{1}{D} \text{Arctan} \left(\frac{1}{a} \sqrt{\frac{\frac{v_m^2}{c_1^2} - 1}{1 - \frac{v_m^2}{c_2^2}}} \right) \right] \quad (3.14)$$

where for $c_1 \leq v_m \leq c_2$, this equation gives real values of κ_{rm1} .

Taking advantage of the fact that $v_m = \frac{\omega}{\kappa_{rm}}$, the corresponding frequency values can be calculated for the given horizontal wavenumber. This is the dispersion relation for the Pekeris waveguide. Figure 7 shows the dispersion curves of the Pekeris waveguide for a few modes.

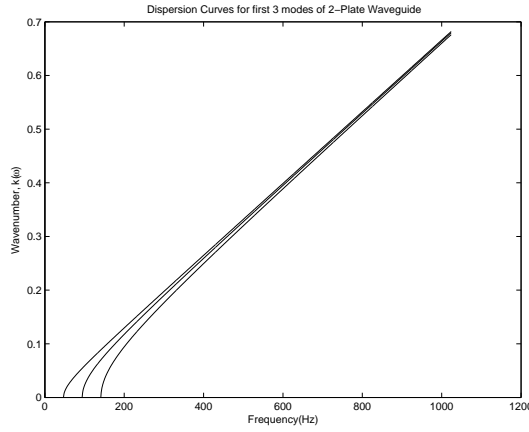


Figure 7: Dispersion Curves for modes 1, 2 and 3 for the Pekeris Waveguide. Model parameters are $c_1 = 1500m/s$, $c_2 = 1800m/s$, $\rho_1 = 1000kg/m^3$, $\rho_2 = 1800kg/m^3$ and $D=75m$.

3.2.2 Phase Velocity and Group Velocity of the Pekeris Waveguide

The group velocity is defined by the derivative of the dispersion relation, $\kappa'(\omega)$, and it is often interpreted as the rate of energy transport from one point to another [26]. This interpretation is very helpful in finding the group velocity for the Pekeris waveguide by considering the energy at various points. The rate of energy transport is defined in the

horizontal direction as the ratio of the mean flux through a vertical section, χ , to the energy density between two such planes a wavelength apart, σv_m .

For a signal, ϕ , the mean flux through a vertical section is

$$\chi = \int_{-\infty}^{\infty} \rho \phi^2 dz$$

and the energy density is

$$\sigma = \int_{-\infty}^{\infty} \frac{v_m}{c^2} \rho \phi^2 dz.$$

Therefore, $u_m = \frac{\chi}{v_m \sigma}$.

For the Pekeris waveguide,

$$\chi_m = \frac{\rho_1}{2\kappa_{zm1}} (\kappa_{zm1} D - \cos \kappa_{zm1} D \cdot \sin \kappa_{zm1} D - a^2 \tan \kappa_{zm1} D \cdot \sin^2 \kappa_{zm1} D) \quad (3.15)$$

and

$$\sigma_m = \frac{1}{c_1^2} \frac{\rho_1}{2\kappa_{zm1}} (\kappa_{zm1} D - \cos \kappa_{zm1} D \cdot \sin \kappa_{zm1} D - \frac{c_1^2}{c_2^2} a^2 \tan \kappa_{zm1} D \cdot \sin^2 \kappa_{zm1} D). \quad (3.16)$$

The group velocity for corresponding phase velocities in the Pekeris waveguide is

$$u_m = \frac{\chi_m}{v_m \sigma_m} \equiv \frac{c_1^2}{v_m} \frac{g_{zm2} D (\kappa_{zm1}^2 + a^2 g_{zm2}^2) + a (g_{zm2}^2 + \kappa_{zm1}^2)}{g_{zm2} D (\kappa_{zm1}^2 + a^2 g_{zm2}^2) + a [g_{zm2}^2 + \frac{c_1^2}{c_2^2} \kappa_{zm1}^2]}. \quad (3.17)$$

We can get the group velocity for a particular frequency because we have the phase velocity associated with that frequency. We are capable of getting $\omega_m(\kappa)$, $v_m(\omega)$ and $u_m(\omega)$, as shown in Figure 8.

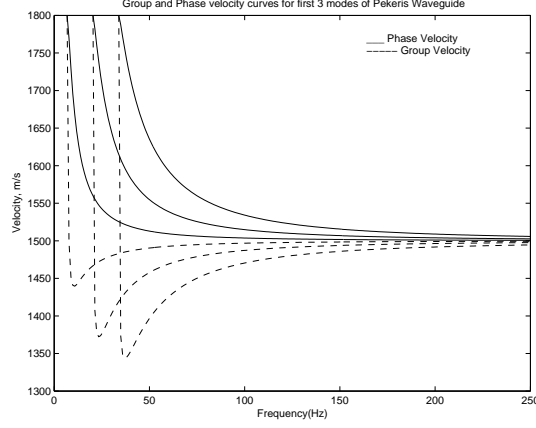


Figure 8: Group and Phase velocity Curves for modes 1, 2 and 3 for the Pekeris Waveguide, Model parameters are $c_1 = 1500m/s$, $c_2 = 1800m/s$, $\rho_1 = 1000kg/m^3$, $\rho_2 = 1800kg/m^3$ and $D=75m$.

3.2.3 Cut-off for frequencies propagating in the Pekeris Waveguide

The equation for the horizontal wavenumber of the wave gives an indication of the range of the frequencies that can propagate through the water medium.

$$\kappa_{rm1} = \frac{1}{\sqrt{\frac{v_m^2}{c_1^2}}} \left[\frac{m\pi}{D} - \frac{1}{D} \text{Arctan} \left(\frac{1}{a} \sqrt{\frac{\frac{v_m^2}{c_1^2} - 1}{1 - \frac{v_m^2}{c_2^2}}} \right) \right]$$

As the phase velocity tends towards the speed of sound in the underlying fluid, $v_m \rightarrow c_2$, the second term in the bracket tends to $\frac{\pi}{2D}$, corresponding to the m^{th} mode low-frequency cut-off,

$$\omega_{om} = \kappa_{rm} = \left(m - \frac{1}{2}\right) \frac{c_1\pi}{D} \sqrt{\frac{1}{1 - \left(\frac{c_1}{c_2}\right)^2}}. \quad (3.18)$$

No frequency components below this value can propagate through the waveguide. Usually, the cut-off value for a mode in the Pekeris waveguide is larger than that for the 2-plate waveguide. Figure 9 shows the cut-off for different modes at varying depths for the 2-plate and Pekeris waveguides. On the other hand, as the phase velocity tends towards the speed of sound in water, $v_m \rightarrow c_1$, the Pekeris waveguide behaves exactly like the perfect waveguide.

At this point, the frequency values are large. At large frequency values, the Pekeris and 2-plate waveguide have the same characteristics.

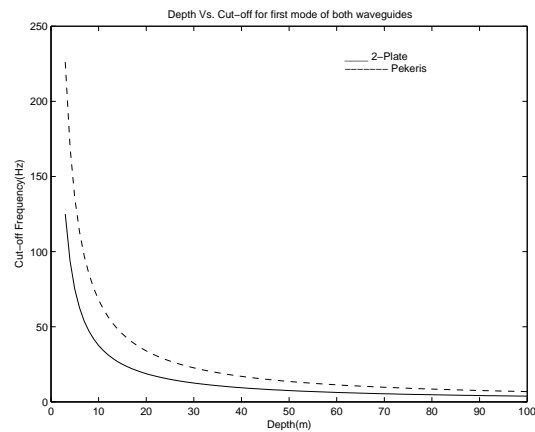


Figure 9: Cut-off as function of Depth for mode 1 of the 2-Plate and Pekeris Waveguide

4.0 IMPLEMENTATION OF WAVEGUIDE MODELS

From observing the spectrograph of sound propagating through water at different distances from the source, one notices a drastic change in the spectrograph, as shown in figure 1. At these different distances we are interested in the local (conditional) moments, such as the mean time and standard deviation from the mean, for a given frequency.

The local mean time, or the average time for a given frequency, at a distance r from the source is:

$$\langle t \rangle_{\omega,r} = \int tP(t|r,\omega)dt = \frac{\int tP(t,\omega)dt}{\int P(t,\omega)dt} = \frac{\int tP(t,\omega)dt}{P(\omega)}. \quad (4.1)$$

where $P(t,\omega)$ is the time-frequency distribution of the signal. The spread from the average time for a given frequency at r can be obtained from

$$\Delta T_{\omega,r}^2 = \langle t^2 \rangle_{\omega,r} - \langle t \rangle_r^2. \quad (4.2)$$

It can be shown that, the spread from the average value of time for a given frequency is invariant to dispersion [18],

$$\Delta T_{\omega,r}^2 = \Delta T_{\omega,0}^2. \quad (4.3)$$

The global and local moments are related by the following expressions [7].

$$\begin{aligned} \langle t \rangle_r &= \int \langle t \rangle_{\omega,r} P(\omega) d\omega \\ \Delta T_r^2 &= \int \Delta T_{\omega,r}^2 P(\omega) d\omega + \int (\langle t \rangle_r - \langle t \rangle_{\omega,r})^2 P(\omega) d\omega. \end{aligned}$$

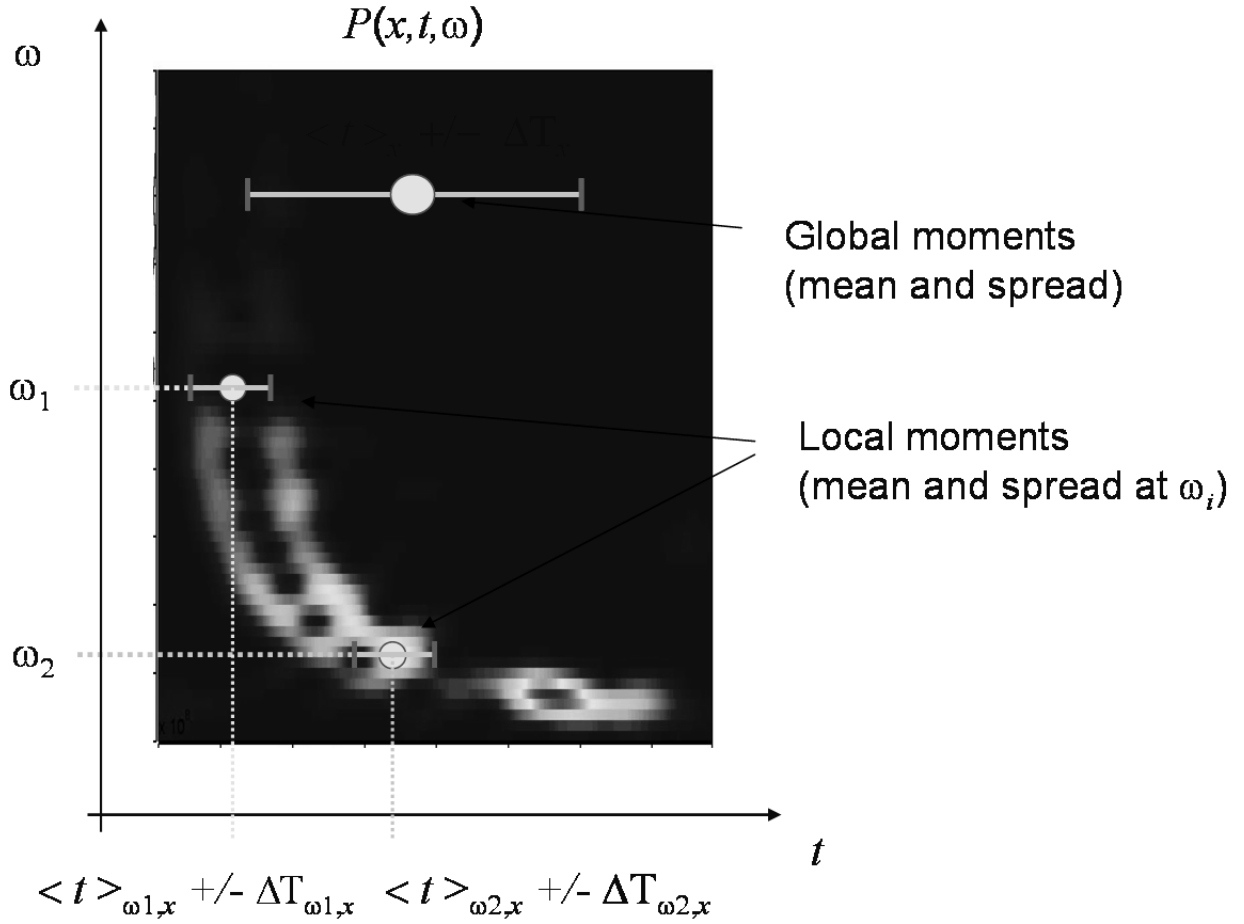


Figure 10: The local and global moments of the spectrum of a signal

4.1 DISPERSION-BASED MODEL FOR PROPAGATION OF SOUND THROUGH WATER

Recall that for any dispersion relation, $\omega = \omega(\kappa) \rightarrow \kappa = \kappa(\omega)$, the group velocity and the group slowness for any frequency per mode are respectively

$$u_m(\kappa) = \frac{\partial \omega}{\partial \kappa} = \omega'(\kappa)$$

$$z_m(\omega) = \frac{\partial \kappa}{\partial \omega} = \kappa'(\omega).$$

The group slowness is the inverse of the group velocity and its use will be more convenient because it directly includes the frequency while the group velocity uses the wavenumber.

The transit time or time of travel is $\kappa'(\omega) \times \text{distance}$ [7]. The conditional mean time for a wave propagated to a distance r from the source is [8],[9]:

$$\langle t \rangle_{\omega,r} = \langle t \rangle_{\omega,0} + \kappa'(\omega)r. \quad (4.4)$$

Let's consider two simple cases. First, for a signal propagating in a non-dispersive medium, the dispersion relation is $\kappa = \frac{\omega}{c}$. The group slowness is simply $\kappa'(\omega) = \frac{1}{c}$ and the conditional mean time after propagating a distance r from the source is

$$\langle t \rangle_{\omega,r} = \langle t \rangle_{\omega,0} + \frac{r}{c}$$

With dispersionless propagation, the spectrum of the signal does not change shape as it propagates and all frequency components are shifted in time by the same amount.

For the second case, consider a signal propagating through a 2-plate waveguide, for which the dispersion relation is $\kappa(\omega) = \frac{1}{c}\sqrt{\omega^2 - \omega_{0m}^2}$. The group slowness per mode for a given frequency is $\kappa'(\omega) = \frac{1}{c}\sqrt{\frac{\omega^2}{\omega^2 - \omega_{0m}^2}}$. Now the transit time varies with frequency and the conditional mean time for the wave after propagating through distance r is:

$$\langle t \rangle_{\omega,r} = \langle t \rangle_{\omega,0} + \frac{r}{c}\sqrt{\frac{\omega^2}{\omega^2 - \omega_{0m}^2}}.$$

The ideas presented above give support for modeling the ocean as a dispersive waveguide, i.e. considering dispersion as the main propagation characteristic. For any dispersion relation we can predict the position in time for all the frequency components present in the wave. Consider an impulse signal; ideally this signal would have all frequencies present in its spectrum. To predict the form of the signal after it has propagated through a distance, we would have to shift all frequency components by the transit time. High frequencies would have the same shape as they did at the source but lower frequencies would spread out. We note that the first conditional moment, $\langle t \rangle_{\omega}$, of many time-frequency distributions equals the group delay, $-\psi'(\omega)$, of the signal. This fact enables us to simulate the nonstationary effects of dispersion by filtering.

Our approach is to design an "Ocean filter" to filter the initial signal by the impulse response of the waveguide to determine the form at a distance. This filter will be a spatially dependent filter whose characteristics will change with the range.

The dispersion relation gives us the group delay as a function of frequency,

$$t_g(\omega) = r\kappa'(\omega) \quad (4.5)$$

For an impulse input, this gives the group delay of the impulse response of the waveguide/filter at r . The phase of the filter representing the waveguide is

$$\psi(\omega) = - \int_0^\omega r\kappa'(\omega')d\omega' = -r\kappa(\omega).$$

Therefore the resulting filter is of the form

$$\begin{aligned} H(\omega; r) &= |H(\omega)|e^{j\psi(\omega)} \\ h(t; r) &= \int |H(\omega)|e^{j\psi(\omega)}e^{j\omega t}d\omega. \end{aligned}$$

Assuming that the attenuation is constant for all frequencies, the magnitude of the frequency is constant and would scale the amplitude of the initial signal.

For the 2-plate waveguide, the group delay is

$$t_g(\omega) = \frac{r}{c} \sqrt{\frac{\omega^2}{\omega^2 - \omega_{0m}^2}},$$

so the frequency response of the waveguide at r is

$$\psi(\omega) = -\frac{r}{c} \sqrt{\omega^2 - \omega_{0m}^2}.$$

The amplitude and phase of the frequency response of the waveguide of depth 50m at 10km is shown in Figure 11 .

Although it is more complicated than the 2-plate waveguide, the same procedure is used to get the frequency and impulse response of the Pekeris waveguide.

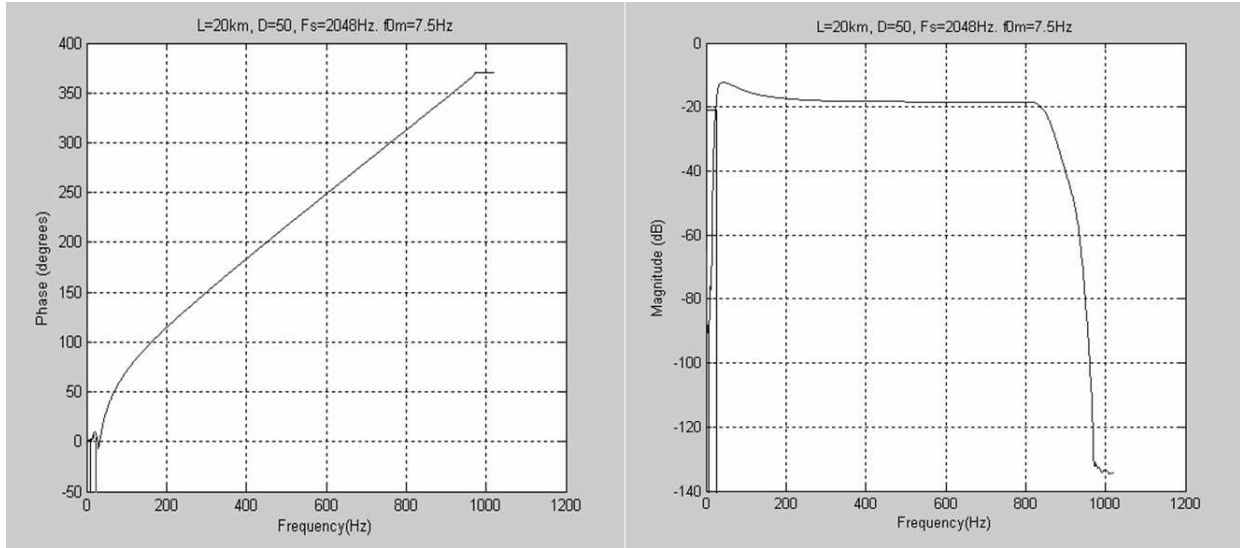


Figure 11: Frequency response of 2-plate waveguide of depth 50m at 10km

4.2 COMPENSATION FOR DISPERSION

In the same way that we can model the ocean as a dispersive waveguide via a filter, we can compensate for dispersion in signals that have propagated through the ocean. There are two approaches to doing this. The first approach ([1],[12],[19]) is to shift the frequency components in the spectrum of the signal by the corresponding group delay. This approach is based on using the time-frequency distribution of the signal. A more convenient method is used in our second approach. In this method, we design a filter a group delay that is the negative of that of the waveguide. The effect this filter has on a signal is that it shifts the frequency components of the signal back by the corresponding group delay of the dispersive channel. The latter is the approach that we have implemented.

The filter that we use to compensate for dispersion in a signal that has been propagated through water for a distance r has the frequency response and impulse response, respectively,

$$H_r^*(\omega; r) = |H_r(\omega; r)|e^{-j\psi(\omega)} \quad (4.6)$$

$$h(-t; r) = \int |H_r^*(\omega)|e^{-j\psi(\omega)}e^{j\omega t}d\omega \quad (4.7)$$

The compensated signal is then obtained by convolving the received signal with $h(-t; r)$.

4.3 IMPLEMENTATION OF WAVEGUIDE MODEL USING MATLAB

MATLAB is a very useful signal processing tool and we have used it to design and apply the required filter. We have modeled the ocean as a dispersive waveguide by designing a filter with specific phase characteristics. The phase characteristics are derived from the dispersion relation of the waveguide.

In filter design, you have the option of choosing between an Infinite Impulse Response (IIR) filter and a Finite Impulse Response (FIR) filter. Using FIR filters, one is able to specify magnitude and phase response characteristics of the filter. IIR filter design allows for the specification of only the magnitude response of the filter and gives a random linear phase. We have implemented FIR filters here because the phase is the more important feature of the filter that we are interested in. Also, FIR filters are stable but we need to check for stability in IIR filters.

Traditionally, one specifies pass-bands and phase intervals in MATLAB to give numerator and denominator coefficients for a particular magnitude and phase response. But because of the complexity of the phase response here, we opt for other methods. By using the Fast Fourier Transform (FFT) command in MATLAB, we derive the coefficients of the waveguide filter after specifying the desired magnitude and phase for the filter in the frequency domain. We then use these derived coefficients for the time domain processing of the signal. The specifications of the filters are given in the following sections.

4.3.1 2-Plate Waveguide

Signals propagating through the 2-plate waveguide are represented in the Frequency domain as

$$Z(\omega) = B(\omega)e^{j\psi(\omega)}. \quad (4.8)$$

The frequency response of the waveguide filter for propagating a signal through a distance r is:

$$\psi(\omega) = -\frac{r}{c}\sqrt{\omega^2 - \left(\frac{m\pi c}{D}\right)^2} = -\frac{r}{c}\sqrt{\omega^2 - \omega_{0m}^2}.$$

The filters are discrete filters and so the analog specifications have to be normalized by the sampling frequency of the signal. The sampling frequency is given as at least twice the magnitude of the highest frequency present in the signal. The default value is 2048 Hz, as this was the sampling rate of some real ocean data we used to compare the simulation against. After normalization, we have the phase response for a discrete filter with the same characteristics as the analog filter.

The magnitude of the filter is not constant for all frequencies, but is rather bandpass. We have tapered the magnitude at lower and higher frequencies to account for sharp discontinuities at the cut-off frequency.

The inputs to the script, given in appendix A, are:

- x: Input signal (Signal at the source).
- c: The sound speed in the ocean channel, in m/s; default: 1500m/s.
- D: Depth of the water column, in meters; default: 100m.
- L: the distance of propagation from the source, in meters; default: 20km.
- m: Propagating mode; default: 1.
- Fs: Sampling frequency of the input, in Hz; default: 2048Hz.

After the user specifies all the available input values, the impulse response, $h(t)$, and the output signal, $y(t)$, are given as the outputs.

The figures 12 - 14 show the time-frequency distribution of the impulse response of the filter at a depth of 3m, 10m and 50m respectively at a distance of 10km and for the default speed of sound ¹.

4.3.2 Pekeris Waveguide

The phase of the frequency response of the Pekeris waveguide, $\psi(\omega)$, is not as easy to derive as in the case of the 2-plate waveguide. One complication is the indirect nature of the dispersion relation. There is no expression that relates the group velocity and the frequency. Another complication to the derivation of the phase is that the frequency values we get from

¹Assuming an impulse as the signal at the source, this is also the time-frequency distribution of the signal at 10km

the series of equations are not equally spaced and neither is the group velocity array. This unequal spacing of the frequency values gives an improper transformation of the analog filter to the discrete filter.

In the script for the modeling of the Pekeris waveguide, given in appendix B, the following are the input parameters.

- x : Input signal.
- c_1 : Sound speed in the Ocean channel, in m/s; default: 1500 m/s.
- c_2 : Sound speed in the underlying fluid, in m/s; default: 1800 m/s.
- ρ_1 : Density of water column, in kg/m^3 ; default: 1000 kg/m^3 .
- ρ_2 : Density of underlying fluid, in kg/m^3 ; default: 1800 kg/m^3 .
- D : Depth of the water column, in meters; default: 100 m.
- L : the distance of propagation from the source, in meters; default: 20 km.
- m : Propagating mode; default: 1.
- F_s : Sampling frequency of the input, in Hz; default: 2048 Hz.

Initially, we have phase velocity values that range from the speed of sound in the water medium to the speed of sound in the underlying fluid. We calculate the corresponding values of frequency and from these values get the group velocity as a function of frequency. The phase of the frequency response of the filter at a distance r from the source is calculated from the following expression

$$\psi(\omega) = -r \int_0^\omega \frac{1}{u_m(\omega')} d\omega'. \quad (4.9)$$

The direct implementation of this phase in a discrete filter will result in an incorrect representation of the desired analog filter. As stated earlier, this is a consequence of the unequal spacing between the derived frequencies. To resolve this complication, we perform a spline interpolation of the values of frequency and their corresponding group velocity values. To do this, we use the unequally spaced values of the frequency, Ω_1 , along with the group velocity, u_{1m} , and specify another array of equally spaced frequency values, Ω_2 , ranging from the lowest frequency, ω_{0m} , to the highest frequency. For values in Ω_2 , we interpolate values of u_{1m} to get values if u_{2m} that correspond to equally spaced frequency values.

Using these new values of group velocity in equation (4.9), the proper phase for the frequency response of the discrete filter is derived.

The plot on the right side of Figure 14 shows the simulation of the propagation of an impulse signal at 10 km in a Pekeris waveguide of depth 50m and other default settings.

4.4 COMPARING THE 2-PLATE AND THE PEKERIS WAVEGUIDES

Although the two models are idealized, they have a few similarities and some very unique characteristics. One similarity is observed in the phase velocity curves of the waveguides for the same input parameters. The phase velocity and group velocity in both waveguides converge to the speed of sound in the water column at high frequencies. However, the group velocity curves are different, especially at lower frequencies. For one, the group velocity in the 2-plate waveguide is never larger than the speed of sound in the water column, c_1 . The group velocity of the pekeris waveguide starts above c_1 at the speed of the bottom, c_2 , dips below c_1 and then converges to c_1 ².

The differences between the two waveguides are only noticeable at short depths ($< 35m$). This is shown using time-frequency distributions of the impulse responses of the waveguides. At short depths, notice how the spectrum looks identical at higher frequencies but are very different at the lower frequencies. The spectrum of the 2-plate waveguide hooks from left to right as the frequency decreases, showing normal dispersion. The spectrum of the pekeris waveguide shows an aberration from normal dispersion. In particular, unlike in the 2-plate waveguide, the lowest frequencies are not always the slowest in the Pekeris waveguide.

At greater depths depths of propagation, the differences between the two waveguides diminish and they become very similar. The spectrograph of the impulse response of the two waveguides are almost indistinguishable. One reason for this is that absorption of energy by the sea floor becomes less of a factor as the sea depth increases and so the sea floor is almost perfectly reflecting. Therefore the (imperfect) Pekeris waveguide approximates the 2-plate waveguide at greater depths. Figures 12-14 show the two waveguides at different depths and distances. Above 50m of depth, the waveguides are very similar.

²see time-frequency distribution

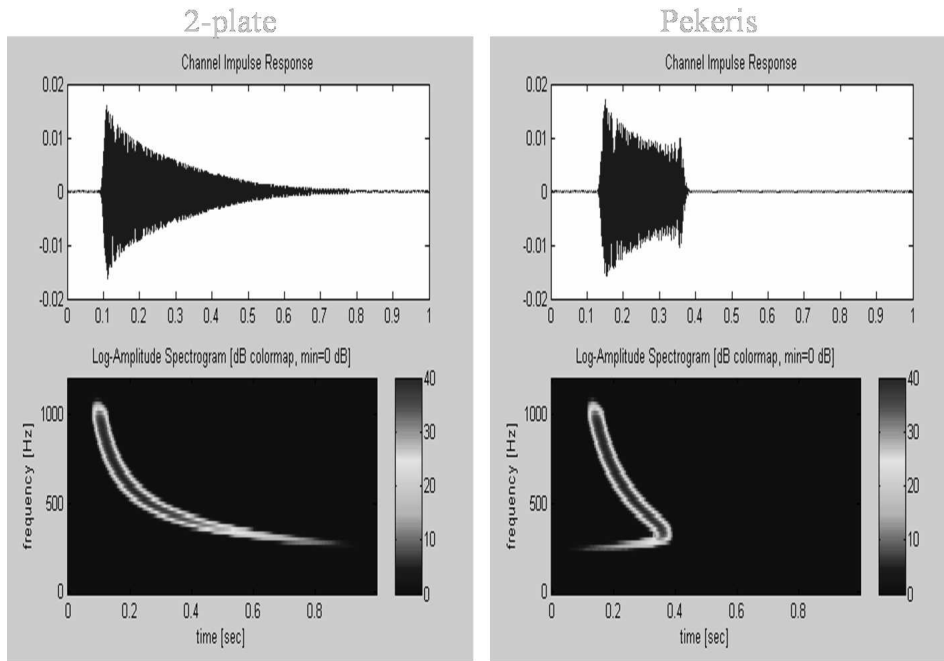


Figure 12: Spectrograph of Pekeris Waveguide and 2-Plate Waveguide at depth of 3m

The cut-off for frequency components that can propagate through the waveguides are different. Sometimes they differ by a factor of 3. The implication is that a lot less frequency components would be able to propagate through the pekeris waveguide than in the 2-plate waveguide for shallow depths. Figure 15 below shows how the cut-off frequency varies with depth for the 2 models.

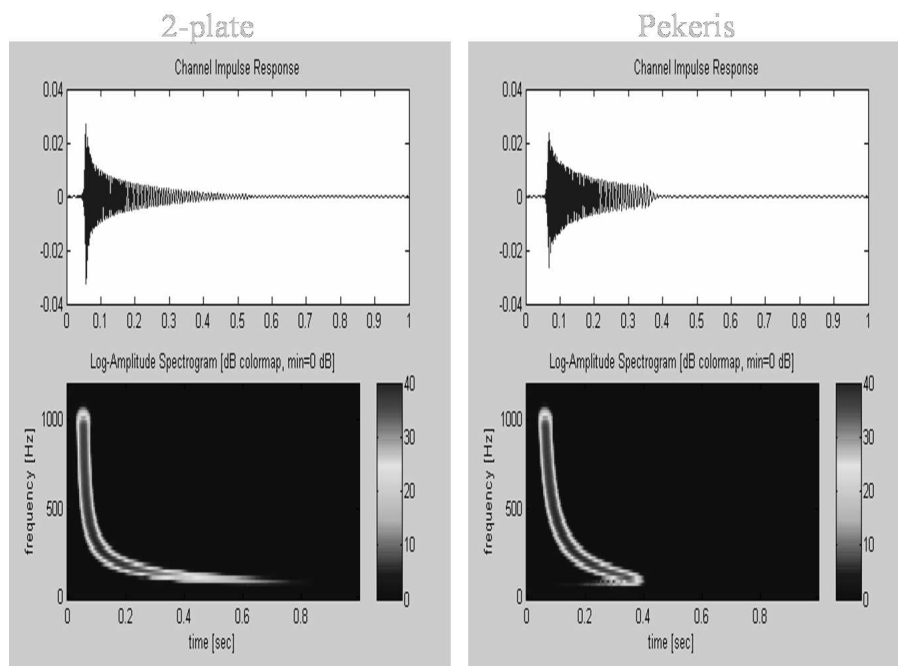


Figure 13: Spectrograph of Pekeris Waveguide and 2-Plate Waveguide at depth of 10m.

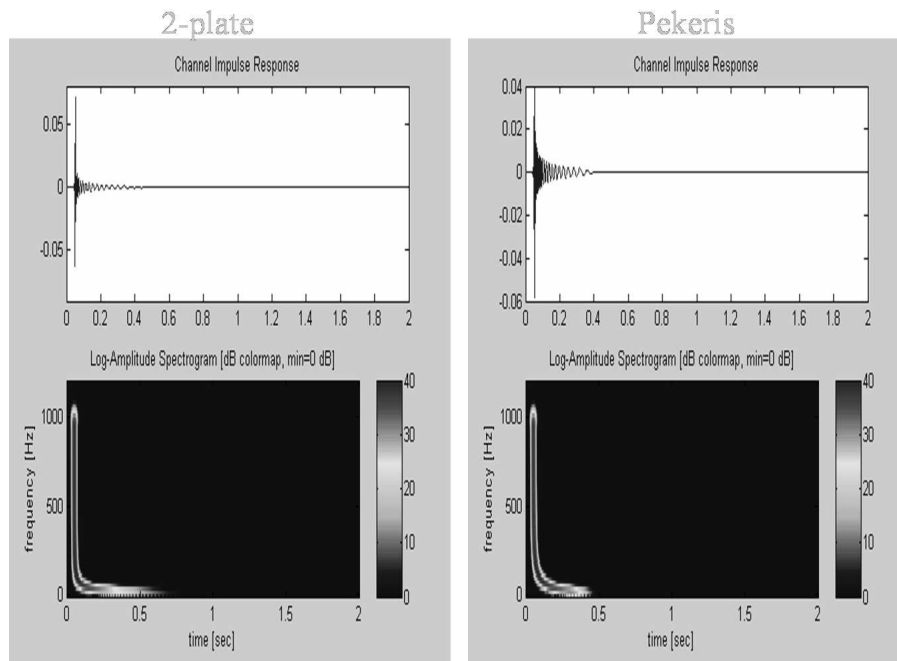


Figure 14: Spectrograph of Pekeris Waveguide and 2-Plate Waveguide at depth of 50m.

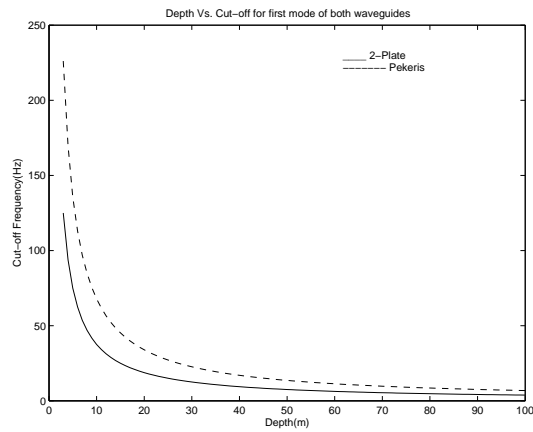


Figure 15: Cut-off frequency vs. Depth for 2-plate and Pekeris waveguides.

5.0 APPLICATION OF MODELS TO SONAR DATA

The filters for the waveguides that we have implemented are applied here to signals recorded in the Yellow Sea by researchers at the Applied Physics Laboratory at the University of Washington. The initial sound signal at the source was an explosion, which is like an (imperfect) impulse. The reason for the double pulse is a secondary explosion called the bubble explosion caused by air bubbles formed from the initial explosion. The signals were recorded at 9 km, 19 km and 38 km from the source of the explosion. As shown in earlier sections, the propagating signal changes significantly with distance. We aim to compensate for the dispersive effects of the shallow ocean channel by processing the signals with the waveguide model filters so that the signals at the different distances are similar.

We do not expect exact agreement with measured data because there are many simplifications in the waveguide models. For example, the sound speed profile of the Yellow Sea channel in which the data were recorded is not isovelocity but varies with depth as shown in figure 16. The models that we implemented have isovelocity sound-speed profiles in which the speed of sound in the water column was taken as $c_1 = 1530m/s$, and the speed of sound for the bottom was $c_2 = 1600m/s$ in the Pekeris waveguide model. We also took the ratio of the densities of the bottom to the water to be $\frac{\rho_2}{\rho_1} = 2.9$, which is a very hard bottom. This ratio was chosen by trial and error to obtain the most suitable match between the model waveforms and the measured data.

Comparison of the spectrographs of the measured data and the simulated waves is shown in figure 17. The figure shows the spectrograph of the measured data at the different distances on the top row and the spectrograph of the simulated waves on the bottom row. The simulated waves show generally good agreement with the experimental measurements.

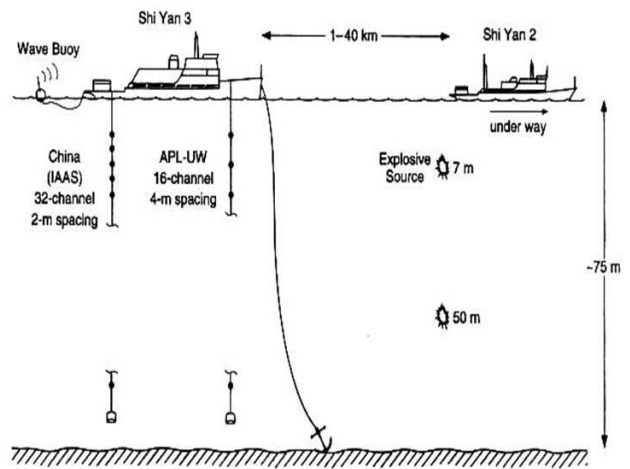
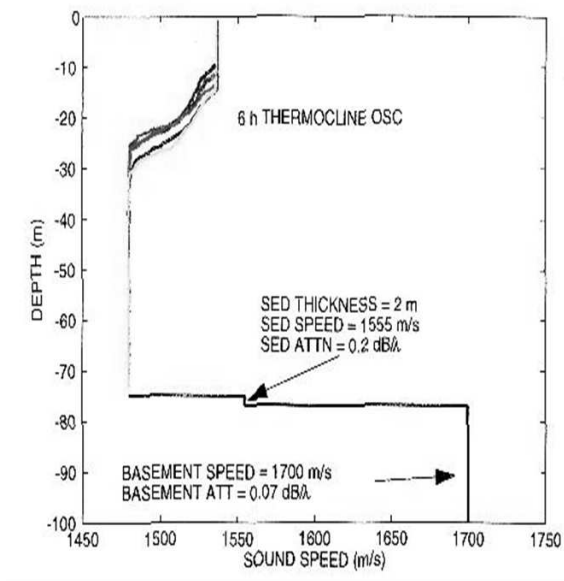


Figure 1. Experimental configuration for the Yellow Sea sound propagation study. Note that 7 m and 50 m correspond only to the preset detonation depths and not to the measured detonation depths. Exact depths for the elements of the APL-UW array are given in figures showing data.

Figure 16: Speed profile for Yellow sea and experimental setup for measurements of data.

We then used the model to process the measured data by filtering it to compensate for the effects of dispersion caused by the water channel on the propagating sound signal as described in the previous chapter. Plots in Figure 18 compare the recorded signals before and after this filtering.

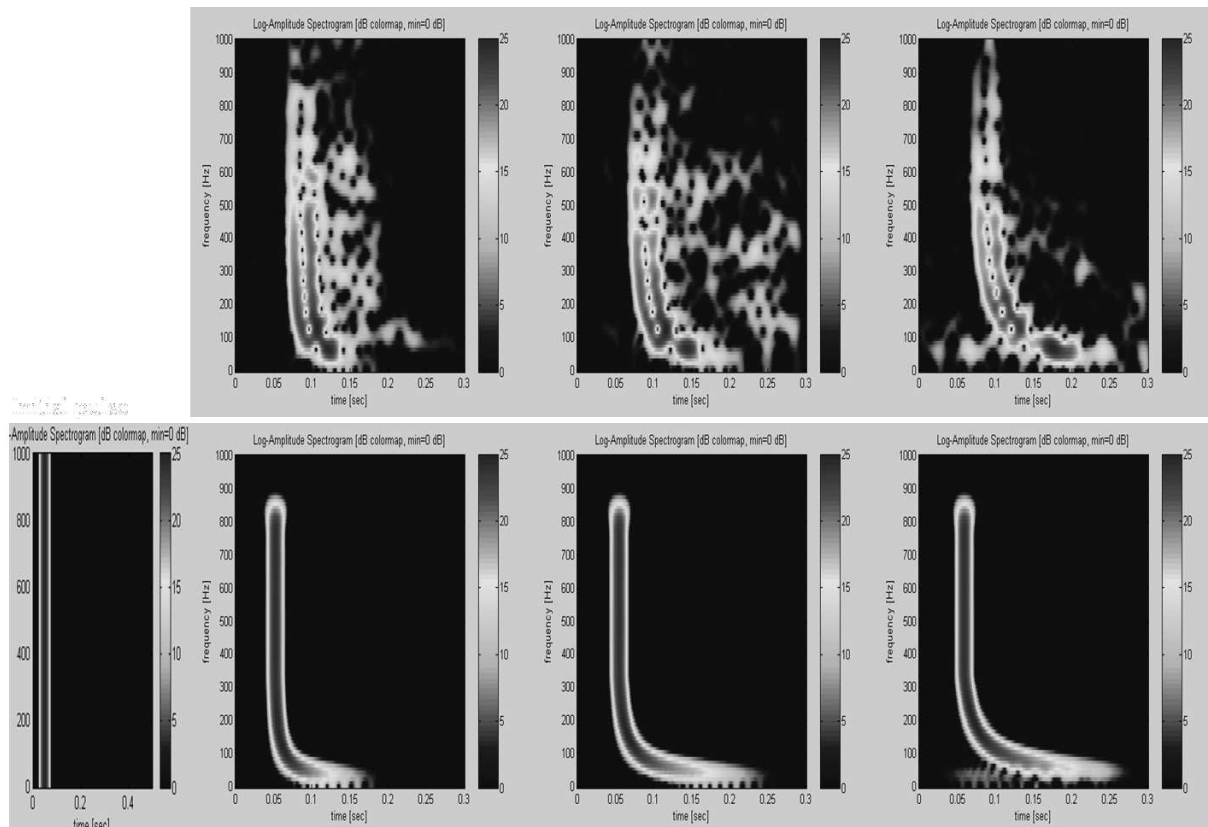


Figure 17: Comparing signals recorded at sea with simulated signals for the Pekeris waveguide: The double pulse in the measured data is caused by air bubbles formed from the initial explosion

Figure 19 shows the time signals of the explosion recorded at sea along with the filtered output. After the signals at the different distances are processed, there are distinguishable bubble pulses that can be noticed in the resulting signal. These bubble pulses that are visible in the initial time series at the source were not as clearly observed in the time series of more distant measurements, but become more evident after the filtering to compensate for dispersion.

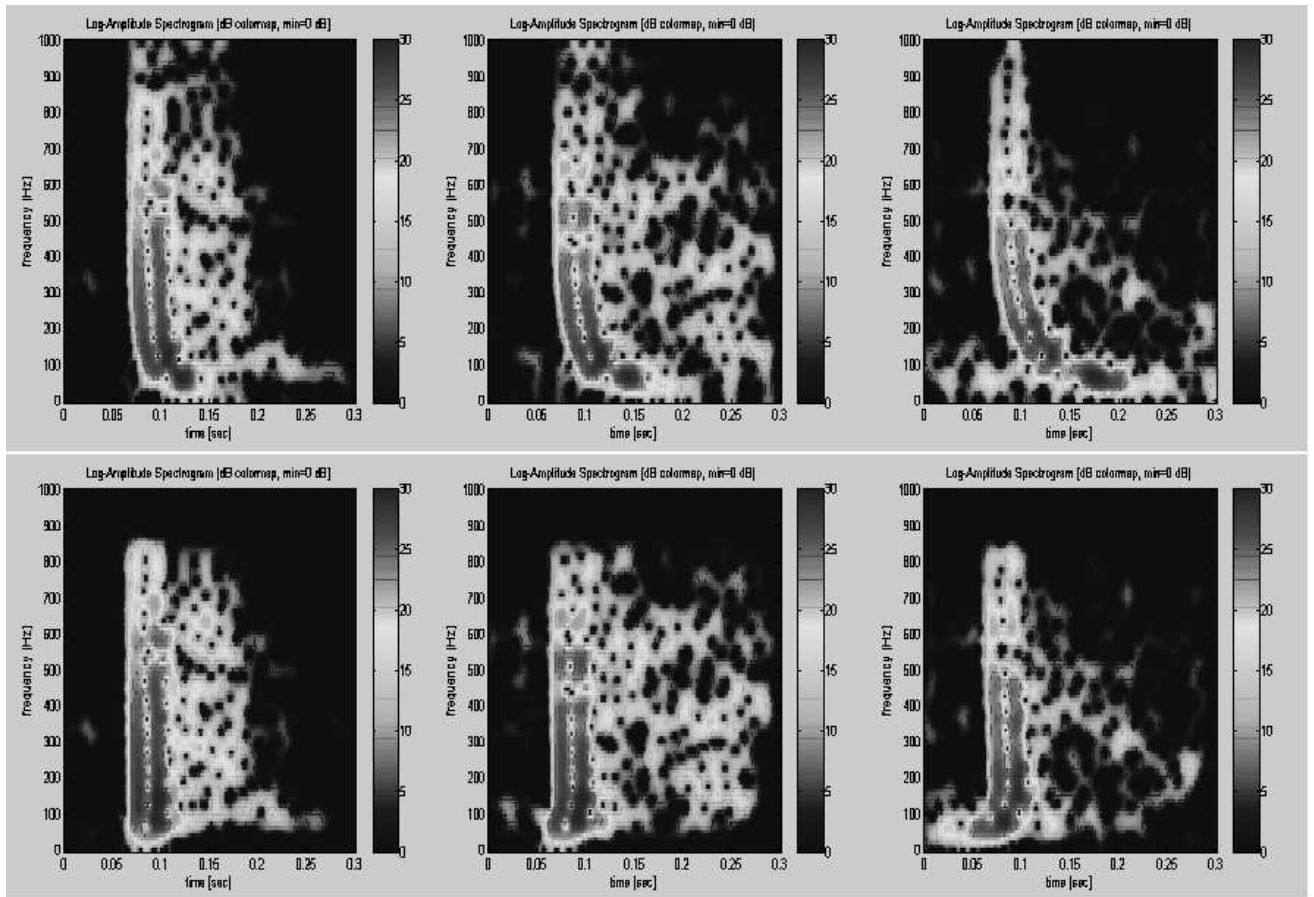


Figure 18: Comparing signals recorded at sea with the corresponding filtered signal for the Pekeris waveguide

The accuracy of the simulation decreases as the distance of propagation increases. This is in accordance with initial intuition. One would have to consider many more factors in the long range propagation such as noise effects. Also, the longer the wave propagates the more prone it is to be distorted by dispersion and noise. Hence, mismatches between the model and the actual environment are accentuated with increased propagation. Work will be done in the future to integrate and reduce noise effects([5],[17]), along with dispersive and other effects, in the propagation of sound in shallow water.

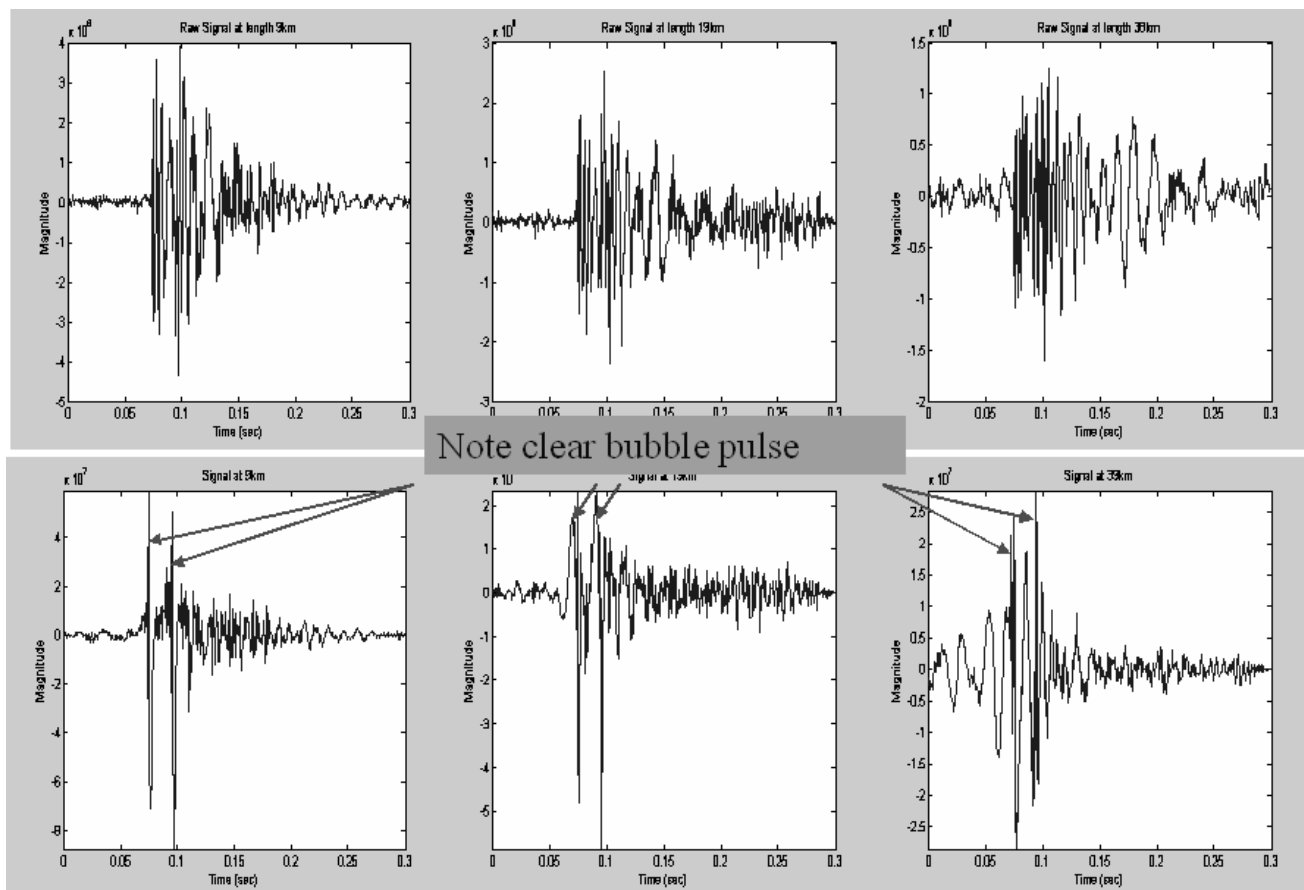


Figure 19: Comparing signals recorded at sea with the corresponding filtered signal for the Pekeris waveguide (Recorded signals above and the filtered signals below: The bubble pulse is clearly evident in the time-series of the filtered data).

6.0 CONCLUSIONS AND FUTURE WORK

We have been able to model how an impulsive sound propagates through water using very few environmental properties of the ocean. The local moments derived from the simple waveguide models show good agreement with the real data recorded from an underwater explosion. We can adapt these waveguides to any ocean environment for modeling the propagation of sound. Also, we can quantify and mitigate the dispersive effects of the ocean on the propagation of a signal by filtering the signal.

In the future, we intend to develop these models to account for range dependence (for example see figure 20). We can do this by considering the piece-wise propagation of a signal. The profile of the ocean will be broken up into sections and the signal is propagated from one section into another. The change that occurs within each section is gradual. For example, we'll break the profile of the ocean into sections where depth is approximately constant and consider sound propagating from section 1 with depth d_1 to section 2 with depth d_2 . Each section of the profile will be range-independent while the overall profile would be range-dependent. In addition to this, we can consider mode coupling under the assumption that the energy of a mode in one section transfers completely to the corresponding mode in the next section [14],[20].

To further approximate the propagation of sound in a waveguide-like ocean channel we will consider other factors that affect the properties of the signal such as transmission loss in the form of absorption and spreading. Spreading loss is the weakening of the intensity of a sound signal as it spreads outward from the source. Absorption is a process that involves the conversion of the acoustic energy into heat by the interaction of the signal with the medium in which it propagates. An example of this occurs as the signal reflects from the ocean surface and the ocean floor.

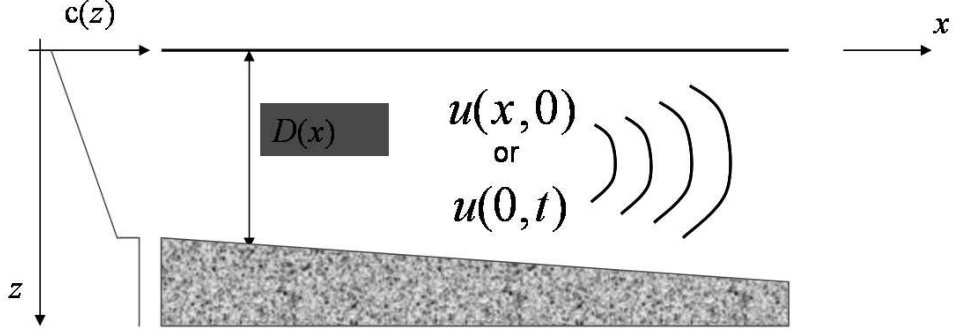


Figure 20: Figure showing example of range and depth dependence: the depth changes with range and the sound speed profile varies with depth.

The losses due to spreading are proportional to the distance traveled [27] and can be quantified by the number of decibels lost per unit distance traveled.

$$\text{Spreading Loss} = 10 \log r \quad (6.1)$$

where r is the distance traveled for the source.

While spreading is dependent only on range, absorption varies with both depth and range. On one hand, absorption loss reduces as the depth increases (inverse proportionality) and on the other hand the absorption loss increases with range. The measure of absorption loss is α , the logarithmic absorption coefficient expressed in decibels per unit distance [27]. For each unit distance traveled, the intensity of the signal reduces by the amount α dB. The expression for the calculation of this parameter as a function of range is given as [27]:

$$\alpha = \frac{10 \log \mathbf{I}_s - 10 \log \mathbf{I}_r}{r} \quad (6.2)$$

where r is the distance propagated by the signal, \mathbf{I}_s is the intensity of the signal at the source and \mathbf{I}_r is the intensity of the signal at r .

The absorption coefficient as a function of depth is [27]:

$$\alpha = \alpha_0(1 - 1.93 \times 10^{-5}d) \quad (6.3)$$

where α_0 is the value at the surface. There are also sources that have derived expressions for the dependence of the absorption coefficient on the propagating frequency.

By considering these factors, the magnitude response of the waveguide filters that we have implemented can be incorporated appropriately, instead of having a constant value for the pass-band. Hence, we would be able to derive a better simulation of the propagating sound signal and also a better approximation of the initial signal from a signal that has traveled through the ocean channel.

Also, we plan to consider local spatial moments and the effects of dispersion on them.

APPENDIX A

MATLAB CODE FOR PEKERIS WAVEGUIDE FILTER

```
function [varargout] = invpekeris(varargin);
%
% USAGE: [h,y] = invpekeris(x,C1,C2,p1,p2,D,L,m,Fs);
%
% Purpose: simulates impulse response of dispersive channel
% (Pekeris waveguide model), then phase conjugates (time-reverses)
% it to inverse filter input x to remove dispersive channel effects.
% To obtain time-reversed impulse response with default parameters,
% call h=invpekeris;
%% To plot impulse response and spectrogram, call without output variables.
%
% Parameters:
% x=input signal vector to be filtered (assumed real). [Default=impulse]
% y=output signal after applying inverse channel filter to x
% h=inverse channel filter (phase-conjugated) impulse response
% C1=sound speed in ocean channel [1500 m/s]
% C2=sound speed in bottom medium [1800 m/s]
% p1=density of water [1000 kg/m^3]
% p2=density of bottom medium [1800 kg/m^3]
% D=depth of ocean channel [100 m]
```

```

% L=propagation distance [10000 m]
% m=mode (default=first [m=1])
% Fs=sampling frequency of x [2048 Hz]
%
% Author: P. Loughlin & D. Aluko, Univ. of Pittsburgh, Dept. of EE
% Created June 5, 2003.
% Adapted from 2-plate waveguide code invwaveguide.m (formerly hookfilter.m,
% originally created by D. Aluko, U. Pittsburgh, 4/20/03)

% Set-up default parameters, then parse inputs
m=1; D=100; L=20000; C1=1500; C2=1800; p1=1000; p2=1800; Fs=2048;
dBrange=40; %dynamic range for log-amp specgram plot
winlen=128; %specram window length;
overlap=fix(0.9*winlen); %window overlap in specgram
NFFT=winlen;
if nargin>1 & ~isempty(varargin{2}), C1=varargin{2}; end
if nargin>2 & ~isempty(varargin{3}), C2=varargin{3}; end
if nargin>3 & ~isempty(varargin{4}), p1=varargin{4}; end
if nargin>4 & ~isempty(varargin{5}), p2=varargin{5}; end
if nargin>5 & ~isempty(varargin{6}), D=varargin{6}; end
if nargin>6 & ~isempty(varargin{7}), L=varargin{7}; end
if nargin>7 & ~isempty(varargin{8}), m=varargin{8}; end
if nargin>8 & ~isempty(varargin{9}), Fs=varargin{9}; end
if nargin>0 & ~isempty(varargin{1})
    x=varargin{1};
else
    x=zeros(1,2*Fs);x(100)=1; %default input = delta(x-100)
end
if (C1>C2),
    txt='Bottom sound speed C2 must be greater than water sound speed C1=';

```

```

        error([txt,num2str(C1),' Hz'])
end

%compute lowest frequency that propagates in Pekeris waveguide
f0m=(m-0.5)*C1*C2/(D*sqrt(C2^2-C1^2))/2; if (2*f0m)>Fs,
    txt='Sampling frequency must be greater than ';
    error([txt,num2str(2*f0m),' Hz for given D, C1, C2']);
end
f0m=f0m/(Fs/2); %Normalize frequency for band-pass and high-pass filter
%design
w0m=2*pi*f0m; %convert to radians (normalized omega restricted to 0-pi)
%Get Pekeris group velocity for given parameters

[w,U,T,k,v,ww]=pekeris_groupvel(length(x),C1,C2,p1,p2,D,m,Fs);
% w -- frequency vector (rad/s) NOTE: equi-spaced. spanning 0-Fs/2;
% ww-- frequency vector (rad/s). spanning w0m-Fs/2;
% U -- group velocity (m/s);
% T -- Angle of incidence (radians)
% k -- Horizontal Wavenumber;
% v -- phase velocity;
dw=w(2)-w(1); % Spacing in frequency vector.
% Check max w to avoid aliasing for given Fs:
ii=(ww/pi<Fs); ww=ww(ii); U=U(ii);
wlen=length(w);
%Normalize w to rad, with max equal to pi
%Integrate 1/U ("group slowness") to get phase corresponding to group delay
ph=-L*cumsum(1./U)*dw; % spectral phase of channel filter model;
pad=length(w)-length(ph); %pad the phase vector with zeros, corresponding to
ph=[zeros(1,pad) ph]; % values of frequency below w0m.
% can't use cumsum since w is not equi-spaced; need to do numerical

```



```

% integration of 1/U taking that into account
ph0=(L/C1)*w; %linear phase to shift h to start at same time, independent of L
B=0.05; %bin-shift factor to compensate for finite-length effects in ifft
ph=ph0+ph-B*w;
H=exp(i*ph); % channel filter freq. response (unit mag);
H=conj(H); %phase conjugate (time-reverse) impulse response for inverse filter
%%h=real(ifft(H,length(x))); %(time-reversed) impulse response;
*** Play with order and cut-off of filter***[B,A]=cheby2(4,3,[1*f0m 0.95]);
    %BPF with lower corner at f0m
[n,Wn]=ellipord([f0m 0.9],[0.9*f0m 0.97],3,40);
[B,A]=ellip(n,3,40,Wn);
[B,A]=butter(4,1/2*f0m,'high');
%impose desired mag freq resp to guard against aliasing, and remove f<f0m.
%h=filtfilt(B,A,h);
[HT,W]=freqz(B,A,wlen);
H=abs(HT').*H; % taper mag in freq. domain to filter against aliasing
fftlens=4*wlen; %forget 2^N; else need to resample h because of zeropadding
h=real(ifft(H,fftlens)); %(time-reversed) impulse response;
h=decimate(h,2); %subsample by 2
[B,A]=cheby2(4,3,f0m,'high'); %high-pass filter above f0m for waveguide
h=filtfilt(B,A,h); %high-pass filter in time domain to attenuate below w0m
h=h-mean(h); % make zero-mean
%taper h in time domain to lessen edge effects
taper=1./(1+exp(-0.01*[1:fix(length(h)/2)]));
taper=taper-min(taper); %normalize min/max to 0/1 respectively
taper=taper/max(taper); taper=[taper fliplr(taper)];
%h=h.*taper;
y=filter(h,1,[x zeros(1,length(h))]); % Output of channel filter;

%plot frequency response and time response of filter

```

```

if nargout>0,
    varargout{1}=h;
else %plot impulse response, output and spectrograms if no output vars
    figure
    subplot(2,1,1),plot([0:length(h)-1]/Fs,fliplr(h)),
    title('Channel Impulse Response')
    subplot(2,1,2)
    hh=[zeros(1,winlen/2) fliplr(h) zeros(1,winlen/2)];
    [B,F,T]=specgram(hh,NFFT,Fs,winlen,overlap);
    B=abs(B).^2/max(max(abs(B).^2));
    logBB=dBrange+10*log10(B);
    logBB=logBB.*(logBB>0); %clip to desired dynamic range
    imagesc(T,F,logBB),axis xy;colorbar
    xlabel('time [sec]'), ylabel('frequency [Hz]')
    title('Log-Amplitude Spectrogram [dB colormap, min=0 dB]')
    figure %plot inverse filtering output
    subplot(2,1,1),plot([0:length(y)-1]/Fs,y),
    title('Output after inverse filtering input x')
    subplot(2,1,2)
    hh=[zeros(1,winlen/2) y zeros(1,winlen/2)];
    [B,F,T]=specgram(hh,NFFT,Fs,winlen,overlap);
    B=abs(B).^2/max(max(abs(B).^2));
    logBB=dBrange+10*log10(B);
    logBB=logBB.*(logBB>0); %clip to desired dynamic range
    imagesc(T,F,logBB),axis xy;colorbar
    xlabel('time [sec]'), ylabel('frequency [Hz]')
    title('Log-Amplitude Spectrogram [dB colormap, min=0 dB]')
end if nargout>1, varargout{2}=y; end return

```

APPENDIX B

GROUP VELOCITY FOR PEKERIS WAVEGUIDE

```
function [varargout]=pekeris_groupvel(varargin)
% Function to compute phase and group velocity of Pekeris waveguide.
%
% USAGE: [w,U,T,k,v,ww]=pekeris_groupvel(len,c1,c2,p1,p2,D,m,Fs);
% Output Parameters:
% w -- frequency vector (rad/s) NOTE: not equi-spaced.
%     e.g., plot(w,U) vs. plot(U) (or note that plot(w) is not
%straight line)
% U -- group velocity (m/s)
%
% Input Parameters:
% len = length of U,w
% c1 = sound speed of water [default: 1500 m/s]
% c2 = sound speed of bottom (c2>c1 for Pekeris) [1800 m/s]
% p1 = density of water [1000 kg/m^3]
% p2 = density of bottom medium [1800 kg/m^3]
% D = depth of ocean channel [100 m]
% m = mode [1]
% Fs = Sampling Frequency [2048 Hz]
```

```
% Author: Dami Aluko, Univ. of Pittsburgh, June 2003.
```

```
%c1=C1; %Sound speed in water, p1=density of water
%c2=C2; %Sound speed in bottom medium, p2=density of bottom medium
% Set-up default parameters, then parse inputs
m=1; D=100; len=1000; c1=1500; c2=1800; p1=1000; p2=1800; Fs=2048;
if nargin>0 & ~isempty(varargin{1}), len=varargin{1}/2; end
if nargin>1 & ~isempty(varargin{2}), c1=varargin{2}; end
if nargin>2 & ~isempty(varargin{3}), c2=varargin{3}; end
if nargin>3 & ~isempty(varargin{4}), p1=varargin{4}; end
if nargin>4 & ~isempty(varargin{5}), p2=varargin{5}; end
if nargin>5 & ~isempty(varargin{6}), D=varargin{6}; end
if nargin>6 & ~isempty(varargin{7}), m=varargin{7}; end
if nargin>7 & ~isempty(varargin{8}), Fs=varargin{8}; end

if (c1>c2),
    error('Bottom sound speed c2 must be greater than water sound speed c1')
end
a=p1/p2;
v=c1:(c2-c1)/len:c2; %phase velocity
k=1/D*((v.^2/c1^2-1).^(-0.5)).*
(m*pi-atan(1/a*(sqrt((v.^2/c1^2-1)./(1- v.^2/c2^2)))));
% wavenumber for horizontal propagation
T=asin(c1./v); %Angle of incidence
w=c1*k./sin(T); %angular frequency
cutoff=(m-0.5)*pi*c1*c2/(D*sqrt(c2^2-c1^2))/pi/2; %lowest frequency that propagates
kz=k.*sqrt(v.^2/c1^2-1); % vertical wavenumber
g=k.*sqrt(1-v.^2/c2^2);
vp=(p1/2./kz).*(kz*D-cos(kz*D).*sin(kz*D)-a^2*tan(kz*D).*(sin(kz*D)).^2);
d=(p1/c1^2/2./kz).*(kz*D-cos(kz*D).*sin(kz*D)-(c1/c2)^2*a^2*tan(kz*D).*
```

```

(sin(kz*D)).^2);
U=vp./(v.*d); %Group velocity for wave
%sort rows in increasing order of frequency
y=[w',U',T',k',v'];
y=sortrows(y);
w=y(:,1)';U=y(:,2)';T=y(:,3)';k=y(:,4)';v=y(:,5)';
% Get rid of the last frequency value (inf) and other corresponding values
w=w(1:length(w)-1);
U=U(1:length(U)-1);
T=T(1:length(T)-1);
k=k(1:length(k)-1);
v=v(1:length(v)-1);
w1=0:pi*Fs/(len-1):pi*Fs; % Frequency spanning 0 to sampling frequency.
w2=0:pi*Fs/(len-1):w(1); % Frequency spanning from 0 to w0m.
w22=0:pi*Fs/(len-1):w(length(w)); % Frequency spanning from 0 to maximum
% calculated frequency (w).
w3=w(length(w)):pi*Fs/(len-1):pi*Fs; % Frequency from max calculated
%frequency(w) to sampling frequency.
w4=(w2(length(w2))+pi*Fs/(len-1)):pi*Fs/(len-1):w(length(w));
%len=length(w1)-length(w2);
ww=w(1):pi*Fs/(len-1):pi*Fs; % Get equispaced values of frequency and the
% corresponding values of the other variables.
len1=length(ww)-length(w3); % length of excess frequency vector.
UU=spline(w,U,ww); % Corresponding group velocity values.
TT=spline(w,T,ww);
kk=spline(w,k,ww);
vv=spline(w,v,ww);
wout=[w2 ww]; % Frequency from 0 to sampling frequency (Equi-spaced).
% Check if group velocity is greater than c1(speed of light in water)
%because of the spline interpolation. If it is, limit it to c1.

```

```

if UU(length(UU))>c1
    UU(length(w4)+1:end)=U(length(U))*ones(1,length(w3));
end

%ww=w(1):(w(length(w))-w(1))/len:w(length(w)); % Get equispaced values of
% frequency and
%Return optional output variables, if any
if nargout>0,
    varargout{1}=wout;
else %plot group and phase velocities against frequency
    figure
    plot(w/2/pi,real(U),'r',w/2/pi,v,'b')
    xlabel('Frequency (Hz)')
    ylabel('Velocities (m/s)')
    Title(['Plot of group- and phase-velocities for Pekeris Waveguide,
        c1=',num2str(c1),', c2=',num2str(c2)])
end
if nargout>1, varargout{2}=UU; end
if nargout>2, varargout{3}=TT; end
if nargout>3, varargout{4}=kk; end
if nargout>4, varargout{5}=vv; end
if nargout>5, varargout{6}=ww; end
return

```

APPENDIX C

MATLAB CODE FOR 2-PLATE WAVEGUIDE FILTER

```
function [varargout] = invwaveguide(varargin);
% USAGE: [h,y] = invwaveguide(x,C,D,L,m,Fs);
%
% Purpose: simulates impulse response of dispersive channel
% (2-plate waveguide model, with rigid bottom and free upper surface),
% then time-reverses (phase conjugates) it to inverse filter input x to
% remove dispersive channel effects.
% To obtain time-reversed impulse response with default parameters,
% call h=invwaveguide2;
% To plot impulse response, output and spectrograms, call without
% output variables.
%
% Parameters:
% x=input signal vector to be filtered (assumed real). [Default=impulse]
% y=output signal after applying inverse channel filter to x
% h=inverse channel filter (phase-conjugated) impulse response
% C=sound speed in ocean channel [1500 m/s]
% D=depth of ocean channel [100 m]
% L=propagation distance [20000 m]
% m=mode (default=first [m=1]; specify m+0.5 to simulate rigid upper surface)
```

```

% Fs=sampling frequency of x [2048 Hz]
%
% Author: P. Loughlin, Univ. of Pittsburgh, Dept. of EE
% Created 5/19/03.
% Adapted from "hookfilter.m," created 4/20/03 by D. Aluko, U. Pittsburgh.

% Set-up default and other parameters, then parse inputs
m=1; D=100; L=20000; C=1500; Fs=2048; %default input parameters
dBrange=40; %dynamic range for log-amp specgram plot
winlen=128; %specram window length;
overlap=fix(0.9*winlen); %window overlap in specgram
NFFT=winlen;
if nargin>1 & ~isempty(varargin{2}), C=varargin{2}; end
if nargin>2 & ~isempty(varargin{3}), D=varargin{3}; end
if nargin>3 & ~isempty(varargin{4}), L=varargin{4}; end
if nargin>4 & ~isempty(varargin{5}), m=varargin{5}; end
if nargin>5 & ~isempty(varargin{6}), Fs=varargin{6}; end
if nargin>0 & ~isempty(varargin{1})
    x=varargin{1};
else
    x=zeros(1,2*Fs);x(100)=1; %default input = delta(x-100)
end
f0m=(m-0.5)*C/(2*D);%lowest frequency that propagates (free upper surface)
if (2*f0m)>Fs,
    txt='Sampling frequency Fs too low; must be greater than ';
    error([txt,num2str(2*f0m),' Hz for specified depth D and speed C']);
end
f0m=f0m/(Fs/2);%normalize by sampling frequency (note max f0m is Fs/2 above)
w0m=2*pi*f0m;%convert to radians (normalized range 0-pi)
dw=2*pi/length(x);

```



```

w=[0:dw:pi]; % normalized frequency range (radians)
wlen=length(w)-1;
w=w(1:wlen); %don't keep both DC and Nyquist
ph=-(L/C)*sqrt(w.^2-w0m^2); % spectral phase of channel filter model;
ph=real(ph); % keep values for w>w0m (w0m is lowest freq. that propagates)
%ph=conj(ph); %mag response will be decaying exponential for w<w0m
B=0.05; %bin-shift factor to compensate for finite-length effects in
% inverse FFT giving noncausal response (if B=0, get wraparound in ifft)
ph0=(L/C)*w; %linear phase to shift h to start at same time, independent of L
ph=(ph+ph0-B*w)*Fs;
H=exp(i*ph); % channel filter freq. response (unit mag);
H=conj(H); %phase conjugate (time-reverse) impulse response for inverse filter
[B,A]=cheby2(8,100,[14.5/8*f0m 0.95]); %BPF with lower corner at f0m
%impose desired mag freq resp to guard against aliasing, and remove f<f0m.
[HT,W]=freqz(B,A,wlen);
H=abs(HT')*.H; % taper mag in freq. domain to filter against aliasing
fftlens=4*wlen; %forget 2^N; else need to resample h because of zeropadding
h=real(ifft(H,fftlens)); %(time-reversed) impulse response;
h=decimate(h,2); %subsample by 2
[B,A]=cheby2(4,60,14.5/8*f0m,'high'); %high-pass filter above f0m for waveguide
h=filtfilt(B,A,h); %high-pass filter in time domain to attenuate below w0m
h=h-mean(h); % make zero-mean
%taper h in time domain to lessen edge effects
taper=1./(1+exp(-0.01*[1:fix(length(h)/2)]));
taper=taper-min(taper); %normalize min/max to 0/1 respectively
taper=taper/max(taper);
taper=[taper fliplr(taper)];
%h=h.*taper;
y=filter(h,1,[x zeros(1,length(h))]); % Output of channel filter;

```

```

%Return optional output variables, if any
if nargin>0,
    varargout{1}=h;
else %plot impulse response, output and spectrograms if no output vars
    figure
    subplot(2,1,1),plot([0:length(h)-1]/Fs,fliplr(h)),
    title('Channel Impulse Response')
    subplot(2,1,2)
    hh=[zeros(1,winlen/2) fliplr(h) zeros(1,winlen/2)];
    [B,F,T]=specgram(hh,NFFT,Fs,winlen,overlap);
    B=abs(B).^2/max(max(abs(B).^2));
    logBB=dBrange+10*log10(B);
    logBB=logBB.*(logBB>0); %clip to desired dynamic range
    imagesc(T,F,logBB),axis xy;colorbar
    xlabel('time [sec]'), ylabel('frequency [Hz]')
    title('Log-Amplitude Spectrogram [dB colormap, min=0 dB]')
    figure %plot inverse filtering output
    subplot(2,1,1),plot([0:length(y)-1]/Fs,y),
    title('Output after inverse filtering input x')
    subplot(2,1,2)
    hh=[zeros(1,winlen/2) y zeros(1,winlen/2)];
    [B,F,T]=specgram(hh,NFFT,Fs,winlen,overlap);
    B=abs(B).^2/max(max(abs(B).^2));
    logBB=dBrange+10*log10(B);
    logBB=logBB.*(logBB>0); %clip to desired dynamic range
    imagesc(T,F,logBB),axis xy;colorbar
    xlabel('time [sec]'), ylabel('frequency [Hz]')
    title('Log-Amplitude Spectrogram [dB colormap, min=0 dB]')
end if nargin>1, varargout{2}=y; end return

```

BIBLIOGRAPHY

- [1] T.J Abatzoglou. A fast local maximum likelihood estimator for time delay estimation. *IEEE Transactions on Acoustics, Speech and Signal Processing*, 34(2), 1986.
- [2] M.J Bastiaans. On the sliding-window representation in digital signal processing. *IEEE Transactions on Acoustics, Speech, and Signal Processing*, pages Vol 33, No4, 1985.
- [3] M.A Biot. Formulation of wave propagation in infinite media by normal coordinates with an application to diffraction. *Journal of the Acoustical Society of America*, pages 381–391, 1957.
- [4] Leon Brillouin. *Wave Propagation and Group Velocity*. Mc-Graw Hill, 1977.
- [5] C.S Clay. Use of arrays for acoustic transmission in a noisy ocean. *Reviews of Geophysics*, 4:475–507, 1966.
- [6] C.S. Clay. Waveguides, arrays and filters. *Geophysics* 31, pages 501–505, 1966.
- [7] L Cohen. *Time-Frequency Analysis*. Prentice Hall, 1995.
- [8] L Cohen. Characterization of transients. *SPIE Proceedings*, 3069:2–15, 1997.
- [9] L Cohen. Pulse propagation in dispersive media. *IEEE SSAP 2000*, pages 485–489, 2000.
- [10] M.L Cowan. Group velocity of acoustic waves in strongly scattering media: Dependence on the volume fraction of scatterers. *The American Physical Society, Physical Review E*, 58, No.5, 1998.
- [11] A.P French. *Vibrations and Waves*. MIT, 1966.
- [12] W.H Haas. A synthesis of frequency domain filters for time delay estimation. *IEEE Transactions on Acoustics, Speech and Signal Processing*, 29(3), 1981.
- [13] Main Iain G. *Vibrations and Waves in Physics*. Cambridge Press, 1978.
- [14] Kuperman Jensen. *Computational Ocean Acoustics*. American Institute of Physics, 1993.

- [15] F.L Kien and K Hakuta. Normal modes and propagation dynamics in a strongly driven raman medium. *The American Physical Society, Physical Review A*, 63, 2001.
- [16] K. Kodera. Analysis of time-varying signals with small bt values. *IEEE Transactions on Acoustics, Speech and Signal Processing*, 26(1), 1978.
- [17] J. F Lingeitch. Time-reversed reverberation focusing in a waveguide. *Journal of the Acoustical Society of America*, 111:6, 2002.
- [18] P. Loughlin and L. Cohen. Time-frequency features invariant to dispersion. *SPIE Defense and Security Symposium*, April 2004.
- [19] Hamid S. Nawab. Signal reconstruction from short-time fourier transform magnitude. *IEEE Transactions on Acoustics, Speech and Signal Processing*,, 31(4), 1983.
- [20] Etter Paul C. *Underwater Acoustic Modeling*. Elsevier Science Publishing, 1991.
- [21] C.L Pekeris. Theory of propagation of sound in a half-space of variable sound velocity under conditions of a shadow zone. *Journal of the Acoustic Society of America*, 18:295–315, 1946.
- [22] C.L Pekeris. Theory of propagation of explosive sound in shallow water. *Geological Society of America*, 27, 1948.
- [23] Slater and Frank. *Electromagnetism*. Mc-Graw-Hill, 1947.
- [24] S.J stanic. Measurements of high-frequency shallow-water acoustic phase fluctuations. *IEEE Journal of Oceanic Engineering*, 25, No.4, 10/2000.
- [25] Ivan Tolstoy. Phase changes and pulse deformation in acoustics. *Journal of the Acoustical Society of America*, 44:675–683, 1968.
- [26] Ivan Tolstoy and C.S. Clay. *Ocean Acoustics: Theory and Experiment in Underwater Sound*. Acoustical Society of America, 1966.
- [27] Robert J. Urick. *Principles of Underwater Sound*. McGraw-Hill,, 3rd edition, 1983.